

Atom-wave diffraction between the Raman-Nath and the Bragg regime: Effective Rabi frequency, losses, and phase shifts

Holger Müller,^{*} Sheng-wei Chiow, and Steven Chu[†]

Physics Department, Stanford University, Stanford, California 94305, USA

(Received 19 April 2007; published 6 February 2008)

We present an analytic theory of the diffraction of (matter) waves by a lattice in the “quasi-Bragg” regime, by which we mean the transition region between the long-interaction Bragg and “channeling” regimes and the short-interaction Raman-Nath regime. The Schrödinger equation is solved by *adiabatic expansion*, using the conventional adiabatic approximation as a starting point, and reinserting the result into the Schrödinger equation to yield a second-order correction. Closed expressions for arbitrary pulse shapes and diffraction orders are obtained and the losses of the population to output states otherwise forbidden by the Bragg condition are derived. We consider the phase shift due to couplings of the desired output to these states that depends on the interaction strength and duration and show how these can be kept negligible by a choice of smooth (e.g., Gaussian) envelope functions even in situations that substantially violate the adiabaticity condition. We also give an efficient method for calculating the effective Rabi frequency (which is related to the eigenvalues of Mathieu functions) in the quasi-Bragg regime.

DOI: [10.1103/PhysRevA.77.023609](https://doi.org/10.1103/PhysRevA.77.023609)

PACS number(s): 03.75.Be, 37.10.Vz, 32.80.Wr, 03.75.Dg

I. INTRODUCTION

A. Background

Diffraction by a point scatters light or matter waves into all directions. A two-dimensional grating produces a few diffraction orders at those angles where the scatter from all of the grating adds coherently. Bragg diffraction by an infinite three-dimensional lattice can produce a single diffraction order, which happens when the scatter from all layers adds constructively, as described by the Bragg condition. When this happens for a higher scattering order (“high-order Bragg diffraction”) virtually all incident radiation can be scattered into this high order, in contrast to the two-dimensional case. By *quasi-Bragg diffraction*, we refer to the intermediate regime where the infinite lattice assumption is no longer valid but approximately true. Using the nomenclature of, e.g., [1], this regime is the transition between the short-interaction Raman-Nath regime and the long-interaction Bragg (weak potential) and “channeling” (strong potential) regimes. In this region, the Bragg condition softens and there may be significant scattering into other than the desired orders. Moreover, couplings between the nonzero diffraction orders may lead to phase shifts of the diffracted waves [2], which is undesirable in many applications.

In this work, we present an analytic treatment of such quasi-Bragg scattering. We will find that by prudent choice of the scattering potential and its envelope function, behavior very similar to Bragg scattering, in particular very low losses and phase shifts, can be obtained for scatterers that substantially violate the assumptions of the simplified theory.

Bragg diffraction famously provides us with the basic knowledge of the structure of crystals, including proteins. It

is also important for many technical applications, such as acousto-optic modulators [3], distributed Bragg reflectors in diode [4] and fiber lasers as well as photonic band-gap crystals [5]. Moreover, Bragg diffraction is a basic method for making surface acoustic wave (SAW) filters in radio frequency technology. In atomic physics, Bragg diffraction is a special case of the Kapitza-Dirac effect [6–10].

Bragg scattering is used as a tool for experiments with Bose-Einstein condensates (BECs) [11–13]. For example, Kozuma *et al.* [14] have shown experimentally that 13 subsequent first-order Bragg diffractions of a BEC can still have good efficiency. More exotic applications include the generation of a collective frictional force in an ensemble of atoms enclosed in a cavity, due to Bragg scattering of a pump light on a self-organized atomic density grating [15], much in the same way as stimulated Brillouin scattering by self-organized acoustic waves in optical fibers [4].

Moreover, Bragg diffraction can act as a beam splitter for matter waves [7,8,11,12,16–20]. The highest-order diffraction so far achieved with matter waves seems to be by Koolen *et al.* [21], who obtained up to eighth-order Bragg diffraction. Atom interferometers based on Bragg diffraction include the one by Giltner *et al.* [22,23], who built a Mach-Zehnder atom interferometer using up to third-order diffraction. Miller *et al.* [24] achieved high contrast in a two-pulse geometry with first-order diffraction and a sufficiently short time between pulses. Torii *et al.* [25] have used first order Bragg diffraction in a Mach-Zehnder geometry with a Bose-Einstein condensate. In addition, Rasel *et al.* [26] have built a Mach-Zehnder atomic-beam interferometer based on Raman-Nath scattering.

More generally, atom interferometers can be used for measurements of atomic properties [27–29], the local gravitational acceleration [30], the gravity gradient, Newton’s gravitational constant [31], tests of the equivalence principle [32] and the fine-structure constant via h/m [33–35]. For planned experiments in space, see [36,37].

While not all the atom interferometers just cited use Bragg diffraction, high-order Bragg diffraction offers several

^{*}holgerm@stanford.edu

[†]Present address: Lawrence Berkeley National Laboratory and Department of Physics, University of California, Berkeley, 1 Cyclotron Road, Berkeley, CA 94720, USA

interesting possibilities for atom interferometers: (i) it makes the atom interact with $2n$ photons at once, which may increase the sensitivity of the interferometer by a factor of n^2 [35] relative to the two-photon transitions. (We note here that other possibilities exist for using high-order transitions in atom interferometers, such as applying multiple low-order pulses [38], operation in the Raman-Nath regime [39] or the magneto-optical beam splitter [40].) (ii) Since Bragg diffraction theoretically allows coherent momentum transfer with an efficiency close to 1, it allows the insertion of many π pulses for additional momentum transfer, which increases the signal in photon recoil measurements [35] (up to $N=30\pi$ pulses based on two-photon adiabatic transfer were used in [33], transferring 60 photon momenta; if these had been fifth-order Bragg pulses, they would have transferred 300). (iii) If losses can be neglected, Bragg diffraction is basically a transition in a two-level system. Thus, many of the techniques developed for standard beam splitters based on Raman transitions can be taken over. For example, several beam splitters addressing different velocity groups, respectively, can be performed simultaneously [35,41].

B. Overview of the existing theory

A summary of the material that is the basis of this work can be found in the textbook by Meystre [16].

A lot of attention has been paid on the theory of the long-interaction time (channeling or Bragg) regimes on the one hand and the Raman-Nath regime on the other hand. Keller *et al.* [1] give a brief account of the most important results. They have been derived using various formalisms: Berman and Bian [9] use a pump-probe spectroscopy picture, focusing on applications as beam splitters in atom interferometers. The phase shift of the diffraction process has been studied by Buchner *et al.* [2], limited to first- and second-order diffraction. Giltner *et al.* [22,23] have reported an atom interferometer based on Bragg diffraction of up to third order and give the effective Rabi frequency in the long-interaction regime, our Eq. (15). A similar derivation was given by Gupta and co-worker [11,12].

While most of this work (as well as ours) is concerned with on-resonance transitions, Dürr and Rempe [42] have considered the acceptance angle (i.e., linewidth) of diffraction. They restrict attention to the case of square-envelope pulses. Wu *et al.* [18] give a numerical study of the latter, again for the case of (a pair of) square pulses. Stenger *et al.* [43] describe the line shape of Bragg diffraction with Bose-Einstein condensates within the Bragg regime.

More general types of diffraction have been studied, such as using chirped laser frequencies [20] in the adiabatic regime where the chirp is sufficiently slow. This regime is similar to Bloch oscillations [44]. Band *et al.* [45] have considered the loss due to atom-atom interactions, which is relevant in experiments with Bose-Einstein condensates (BECs). Blakie and Ballagh [46] explore the use of Bragg diffraction in probing vortices in BECs.

On the other hand, the picture is still incomplete in the quasi-Bragg regime we are concerned with. Dürr, Kunze and Rempe have analytically calculated corrections to the effective

Rabi frequency for large potential depth [47] in the case of second-order scattering with a square envelope function. Champenois *et al.* [48] consider both the Raman-Nath and the Bragg regime using a Bloch-state approach; for the Bragg regime, however, their treatment is restricted to the first diffraction order and square envelopes. Bordé and Lämmerzahl [19] give an exhaustive treatment of square-envelope scattering that is based on matching the boundary conditions at the beginning and end of the pulse. This method, unfortunately, cannot readily be generalized to smooth envelope functions.

The Mathieu equation formalism is a powerful tool for studying diffraction with arbitrary potential depth and interaction times, as demonstrated by Horne, Jex, and Zeilinger [49]. However, similar to the work of Bordé and Lämmerzahl, the Mathieu equation formalism assumes constant envelopes and cannot readily be generalized to smooth envelope functions. As we shall see (and has already been pointed out, see, e.g., [1]), smooth envelope functions are of particular interest because they allow high-efficiency scattering into a single order even in the quasi-Bragg regime. The mathematical properties of the Mathieu functions themselves have been explored by many workers. Of relevance for this work is the power-series expansion of Mathieu functions reported by Kokkorakis and Roumelotis [50].

C. Motivation

In the experimental applications, it is often desirable to make the interaction time as short as compatible with certain requirements on the efficiency and parasitic phase shifts. This can be achieved by operating in the quasi-Bragg regime. For example, in atomic physics, long interaction times increase losses due to single-photon excitation and also systematic effects in atom interferometers. For fifth-order Bragg scattering of cesium atoms in a standing light wave, satisfying the adiabaticity criterion requires interaction times $\gg 0.4$ s, see Sec. I E 2. This exceeds the time available in experiments under freefall conditions, and would give rise to huge losses by single-photon excitation. Moreover, the very sharp Bragg condition in the pure Bragg regime means that scattering happens only if the incident waves are within a very narrow range (much below the recoil velocity) of the velocity distribution of a thermal sample, which may mean that a large fraction will not be scattered at all. However, operation in the quasi-Bragg regime requires a theoretical calculation of the losses and phase shifts encountered, and strategies to minimize them. This is best done by analytic equations for these parameters, which allow one to easily see which parameters have to take which values.

Unfortunately, in this regime the population of the diffraction orders is particularly difficult to calculate [1] and so the existing analytic theory of the quasi-Bragg regime is restricted to square envelope functions or low orders, or both. Moreover, even then, using the known formalisms it is hard to obtain power-series approximations of parameters such as the effective Rabi frequency in terms of the interaction strength.

The aim of this paper is to present an analytic theory of the quasi-Bragg regime that allows the treatment of arbitrary

scattering orders and envelope functions of the scattering potential. To do so, we develop a systematic way of obtaining more and more accurate solutions of the Schrödinger equation that starts from the usual adiabatic approximation. This allows us to calculate the population of the diffraction orders, including losses to unwanted outputs and phase shifts. We can thus specify the minimum interaction time and the maximum interaction strength that yield losses which are below a given level, and consider the influence of the pulse shape. It will turn out that efficient scattering can be maintained with interaction times that substantially violate the adiabaticity criterion, in agreement with experiments [1]. For example, we show that fifth-order scattering of Cs atoms still has negligible losses and phase shifts for interaction times on the order of 10 μ s if the pulse shape of the light is appropriately chosen. This minimum interaction time even decreases for higher scattering order. We will restrict attention to on-resonant Bragg diffraction, neglecting any initial velocity spread that the atoms may have. This can certainly be a good assumption for experiments using Bose-Einstein condensed atoms, but also for a much wider class of experiments: The minimum interaction time that will still lead to low losses will turn out to be roughly given by $1/(n\omega_r)$, where ω_r is the recoil frequency and n the Bragg diffraction order, see Eq. (74). Such short pulses have a Fourier linewidth that is on the order of $n\omega_r$. This means that a velocity spread on the order of the recoil velocity cannot be resolved, even though the velocity selectivity increases $\sim n$ due to the multiple photons scattered. The preparation of atoms having a velocity spread of $1/100$ – $1/10$ of the recoil velocity is standard practice in atomic fountains.

While our theory will be stated in the language of atomic physics, with an eye on applications in atom interferometry, it can be adapted to Bragg diffraction in all fields of physics.

D. Outline

This paper is organized as follows: In Sec. I E, we describe our basic Hamiltonian and the conventional theory for the Bragg and the Raman-Nath regime. In Sec. I F, an exact solution for rectangular envelope functions will be presented that uses Mathieu functions. In Sec. II, we find a general form for the corrections of the effective Rabi frequency which is valid for arbitrary scattering orders. In Sec. III we present our method for calculating the phase shifts and losses, adiabatic expansion. In Secs. IV and V, we consider square and Gaussian envelope functions and give a practical example of high-order Bragg scattering of Cs atoms.

E. Problem

In the remainder of this Sec. I, we define the basic problem and review the basic theory of the adiabatic and the Raman-Nath case (as described, e.g., in [16]) and of the Mathieu equation approach. This is to define the notation and for the reader's convenience. The reader already familiar with this may want to proceed to the following sections, which describe the results of this paper.

Consider scattering of an atom of mass M by a standing wave of light along the z direction. Ignoring effects of spon-

aneous emission, the Hamiltonian describing the interaction of the atoms with the standing wave having a wave number k is (in a frame rotating at the laser frequency ω)

$$H = \frac{p^2}{2M} - \hbar \delta |e\rangle\langle e| + \hbar \Omega_0(t) \cos(kz) (|e\rangle\langle g| + \text{H.c.}), \quad (1)$$

where $[z, p] = i\hbar$ and δ is the detuning. The Rabi frequency Ω_0 may in general be time dependent. For the purpose of this introduction, we will assume it to be constant. In the later sections of this paper, we shall be interested in the effects of different pulse shapes, however. Substituting

$$|\psi(t)\rangle = e(z, t)|e\rangle + g(z, t)|g\rangle \quad (2)$$

into the Schrödinger equation yields the coupled differential equations

$$\begin{aligned} i\hbar \dot{e}(z, t) &= \frac{p^2}{2M} e(z, t) + \hbar \Omega_0 \cos(kz) g(z, t) - \hbar \delta e(z, t), \\ i\hbar \dot{g}(z, t) &= \frac{p^2}{2M} g(z, t) + \hbar \Omega_0 \cos(kz) e(z, t), \end{aligned} \quad (3)$$

where the overdot denotes the time derivative. For large δ compared to the linewidth of the excited state (and thus also $\delta \gg \Omega_0, \omega_r$) and the atoms initially in the ground state, we can adiabatically eliminate the excited state,

$$i\hbar \dot{g}(z, t) = -\frac{\hbar^2}{2M} \frac{\partial^2 g(z, t)}{\partial z^2} + \frac{\hbar \Omega_0^2}{\delta} \cos^2(kz) g(z, t). \quad (4)$$

This equation with its periodic potential is invariant under a translation by an integer multiple of k^{-1} . Applying the Bloch theorem, we can look for solutions having constant quasimomentum; in particular, we can restrict attention to the case of vanishing quasimomentum. For constant Ω_0 , this is a Mathieu equation for which exact solutions are known; this formalism will be described in Sec. I F and developed further in Sec II. If we let

$$g(z, t) = \sum_{m=-\infty}^{\infty} g_m(t) e^{imkz} \quad (5)$$

and use $\cos^2(kz) = \frac{1}{2} + \frac{1}{4}(e^{2ikz} + e^{-2ikz})$, we obtain

$$\begin{aligned} i\hbar \sum_{m=-\infty}^{\infty} \dot{g}_m(t) e^{imkz} &= \hbar \sum_{m=-\infty}^{\infty} [(\omega_r m^2 + \Omega) g_m \\ &+ (\Omega/2)(g_{m+2} + g_{m-2})] e^{imkz}, \end{aligned} \quad (6)$$

where we have introduced the two-photon Rabi frequency

$$\Omega = \frac{\Omega_0^2}{2\delta} \quad (7)$$

and the recoil frequency

$$\omega_r = \frac{\hbar k^2}{2M}. \quad (8)$$

This can only hold if for all m

$$i\hbar\dot{g}_m = \hbar(\omega_r m^2 + \Omega)g_m + \hbar(\Omega/2)(g_{m+2} + g_{m-2}). \quad (9)$$

(Since this equation couples only odd or even momentum states, respectively, we can and will look for solutions that have either the odd or even terms zero. In view of this the use of both even and odd indices may seem unnecessary, but will have advantages when we consider Bragg diffraction.) The theoretical description of Bragg diffraction is relatively simple in the short-interaction limit (the Raman-Nath regime) and in the case of an infinite scatterer, the Bragg regime.

1. Raman-Nath regime

The Raman-Nath regime is defined as the case of very short interaction time, so that the kinetic energy term is negligible against the resulting energy uncertainty. Equation (9) reduces to

$$i\hbar\dot{g}_m = \hbar(\Omega/2)(g_{m+2} + g_{m-2}), \quad (10)$$

which we have simplified by shifting the energy scale by $-\hbar\Omega$. Since these equations only couple states which differ by an even multiple of the momentum $\hbar k$, we can restrict attention to even indices $2m$. They can be satisfied by Bessel functions:

$$g_{2m} = (-i)^m J_m(\Omega t). \quad (11)$$

At $t=0$, this solution has all atoms in the zero momentum state $g_0=1$, $g_{2m \neq 0}=0$. For $t \neq 0$, the probability to find the atom to have a transverse momentum $2m\hbar k$ is $P_{2m}(t) = J_m^2(\Omega t)$. The Raman-Nath approximation holds provided that $t \ll 1/\sqrt{2\Omega\omega_r}$ (because then a high energy uncertainty justifies our neglect of the kinetic energy). Clearly, the transfer efficiency P_{2m} for any particular m is limited. For example, the maximum probability to find the atom in the ground state after scattering two photons is approximately 0.34.

2. Bragg regime

For the Bragg regime, we take into account the kinetic energy term and work in configuration space. We now assume initial conditions $g_{-n}=1$ and $g_m=0$ for $m \neq -n$. To simplify, we subtract a constant offset $n^2\hbar\omega_r + \hbar\Omega$ from the energy scale. Equation (9) now reads

$$\begin{aligned} & \vdots \\ i\hbar\dot{g}_{-n-2} &= (4+4n)\hbar\omega_r g_{-n-2} + \frac{1}{2}\hbar\Omega(g_{-n} + g_{-n-4}), \\ i\hbar\dot{g}_{-n} &= \frac{1}{2}\hbar\Omega(g_{-n+2} + g_{-n-2}), \\ i\hbar\dot{g}_{-n+2} &= (4-4n)\hbar\omega_r g_{-n+2} + \frac{1}{2}\hbar\Omega(g_{-n+4} + g_{-n}), \\ & \vdots \\ i\hbar\dot{g}_{-n+2k} &= 4k(k-n)\hbar\omega_r g_{-n+2k} + \frac{1}{2}\hbar\Omega(g_{-n+2k+2} \\ & \quad + g_{-n+2k-2}), \end{aligned}$$

$$\begin{aligned} & \vdots \\ i\hbar\dot{g}_{n-2} &= (4-4n)\hbar\omega_r g_{n-2} + \frac{1}{2}\hbar\Omega(g_n + g_{n-4}), \\ i\hbar\dot{g}_n &= \frac{1}{2}\hbar\Omega(g_{n+2} + g_{n-2}), \\ i\hbar\dot{g}_{n+2} &= (4+4n)\hbar\omega_r g_{n+2} + \frac{1}{2}\hbar\Omega(g_{n+4} + g_n), \\ & \vdots \end{aligned} \quad (12)$$

Energy conservation will favor transitions from $-n \rightarrow n$, if the processes are sufficiently slow. This is the result of the adiabatic elimination of the intermediate states ($k \neq 0$ and $k \neq n$): If

$$|4k^2 - 4nk|\hbar\omega_r \gg \hbar\Omega, \quad (13)$$

for all $0 < k < n$, we can assume that the k th equation is always in equilibrium with $\dot{g}_{-n+2k} \approx 0$. Then, for example,

$$g_{-n+2} = -\frac{1}{8}\hbar\Omega \frac{1}{(nk-k^2)\hbar\omega_r} g_{-n}. \quad (14)$$

Relations such as this can be used to successively eliminate all $n-1$ intermediate states. With

$$\Omega_{\text{eff}} = \frac{\Omega^n}{(8\omega_r)^{n-1}} \prod_{k=1}^{n-1} \frac{1}{nk-k^2} = \frac{\Omega^n}{(8\omega_r)^{n-1} [(n-1)!]^2}, \quad (15)$$

we obtain

$$\begin{aligned} i\hbar\dot{g}_{-n} &= \frac{1}{2}\hbar\Omega_{\text{eff}} g_n, \\ i\hbar\dot{g}_n &= \frac{1}{2}\hbar\Omega_{\text{eff}} g_{-n} \end{aligned} \quad (16)$$

(where we have removed a constant light shift term). This can be readily solved,

$$g_{-n}(t) = \cos \frac{1}{2}\Omega_{\text{eff}} t, \quad g_n(t) = -i \sin \frac{1}{2}\Omega_{\text{eff}} t. \quad (17)$$

For a time-varying Ω ,

$$\begin{aligned} g_{-n}(t) &= \cos \left(\frac{1}{2} \int_{-\infty}^t \Omega_{\text{eff}}(t') dt' \right), \\ g_n(t) &= -i \sin \left(\frac{1}{2} \int_{-\infty}^t \Omega_{\text{eff}}(t') dt' \right). \end{aligned} \quad (18)$$

This is an exact solution of the adiabatic equations of motion, Eqs. (16), for real Ω_{eff} , as can be verified by insertion. If the integral appearing in the trigonometric functions is equal to π (a “ π pulse”), all of the population ends up in the final state; if it is $\pi/2$ (a “ $\pi/2$ pulse”), half of it.

While operation in the Bragg regime is lossless, it requires relatively long-interaction times. In the previous section, we used the condition $4(1-n)\omega_r \gg \Omega$, which translates into

$$\Omega_{\text{eff}} \ll \frac{8(n-1)^n \omega_r}{2^n (n-1)!^2}. \quad (19)$$

This is $\sim \omega_r$ for $n \leq 5$, but drops rapidly, e.g., $\Omega_{\text{eff}} \ll 2 \times 10^{-4} \omega_r$ for $n=10$.

For later use, we consider the case of complex $\Omega_{\text{eff}} = |\Omega_{\text{eff}}|e^{i\varphi}$, where φ is the argument of Ω_{eff} . Hermiticity then requires us to use Ω_{eff}^* in the second of Eqs. (16). The solution of these equations for constant Ω is $g_{-n}(t) = \cos \frac{1}{2}|\Omega_{\text{eff}}|t$, $g_n(t) = -ie^{-i\varphi} \sin \frac{1}{2}|\Omega_{\text{eff}}|t$. For time-varying complex Ω , the generalization of Eqs. (18) by substituting $|\Omega_{\text{eff}}|$ and inserting the factor of $e^{-i\varphi}$ into $g_n(t)$ is an exact solution for constant φ , and remains approximately valid as $|\dot{\varphi}| \ll |\Omega_{\text{eff}}|/2$, as can be seen by inserting into Eqs. (16). Thus, this solution holds for varying complex Ω_{eff} as long as its argument changes adiabatically. In the following, Ω_{eff} is always understood to be the absolute value unless otherwise stated.

F. Mathieu equation approach

For constant Ω_0 , we can apply the method of separation of variables to Eq. (4). We are looking for a solution of the form

$$g(z, t) = g_t(t)g(z) \quad (20)$$

to obtain

$$\begin{aligned} ig'_t - \omega_t g_t &= 0, \\ -\frac{\hbar}{2M} g'' + 2\Omega \cos^2(kz)g - \omega_t g &= 0, \end{aligned} \quad (21)$$

with ω_t being the separation constant. The second equation is the Mathieu equation. By using $v = z/k$,

$$\begin{aligned} a &= -\frac{\Omega}{\omega_r} + \frac{\omega_t}{\omega_r}, \\ q &= \frac{\Omega}{2\omega_r}, \end{aligned} \quad (22)$$

it can be brought to the standard form

$$g''(v) + [a - 2q \cos(2v)]g(v) = 0. \quad (23)$$

This is an eigenvalue equation in a . The eigenfunctions can be expressed by Fourier series

$$\begin{aligned} \text{se}_{2n+1}(v, q) &= \sum_{r=0}^{\infty} B_{2r+1}^{(2n+1)} \sin(2r+1)v, \\ \text{se}_{2n+2}(v, q) &= \sum_{r=0}^{\infty} B_{2r+2}^{(2n+2)} \sin(2r+2)v, \\ \text{ce}_{2n}(v, q) &= \sum_{r=0}^{\infty} A_{2r}^{(2n)} \cos 2rv, \\ \text{ce}_{2n+1}(v, q) &= \sum_{r=0}^{\infty} A_{2r+1}^{(2n+1)} \cos(2r+1)v. \end{aligned} \quad (24)$$

The eigenvalues associated with the v -even functions ce are denoted a_r , those associated with odd functions se are denoted b_r [51]. Insertion of these series into the Mathieu equation

allows one to determine the eigenvalues and the Fourier coefficients [51,52]. This is tedious, but tables [51] and standard numerical routines allow one to find numerical values easily.

In this paragraph, we use units with $\omega_r = 1$. For an atom initially in a pure momentum state with $p = -n\hbar k$, we express the wave function $\psi(t=0)$ as a series of Mathieu functions:

$$e^{in_v} = \sum_m C_m \text{ce}_m + S_m \text{se}_m. \quad (25)$$

This is possible because the functions ce and se form a complete orthogonal set [51]. The coefficients of the expansion are thus given by the Fourier coefficients of the Mathieu functions. Once they are known, we can write down the amplitude of finding the atom with a momentum n_f at a later time:

$$\begin{aligned} g_{n_f} &= \frac{1}{2\pi} \int_0^{2\pi} e^{-in_f v} \left(\sum_m A_{n_i}^{(m)} \text{ce}_m(v, q) e^{i(a_m+2q)t} \right. \\ &\quad \left. + iB_{n_i}^{(m)} \text{se}_m(v, q) e^{i(b_m+2q)t} \right) dv \\ &= \frac{e^{2iqt}}{2} \left(\sum_m A_{n_i}^{(m)} A_{n_f}^{(m)} e^{ia_m t} + B_{n_i}^{(m)} B_{n_f}^{(m)} e^{ib_m t} \right). \end{aligned} \quad (26)$$

(The $e^{-in_f v}$ has a minus in the exponent because this is a reverse Fourier transform.) While in general this is a very complicated function of t , for low values of q only $B_{n_i}^{(n_i)}$ and $A_{n_i}^{(n_i)}$ will be large. If we neglect all others,

$$|g_{n_f}|^2 \approx \frac{1}{4} [|A_{n_i}^{(n_i)}|^4 + |B_{n_i}^{(n_i)}|^4 \pm 2|A_{n_i}^{(n_i)}|^2 |B_{n_i}^{(n_i)}|^2 \cos(a_{n_i} - b_{n_i})t]. \quad (27)$$

The plus sign is for $n_f = n_i$, the minus sign for $n_f = -n_i$. Thus, the atoms will oscillate between n_i and $-n_i$ with an effective Rabi frequency $\Omega_{\text{eff}} \equiv a_{n_i} - b_{n_i}$.

For an explicit example, let the two photon Rabi frequency be $\Omega = 2q = 3$ for $0 < t < T$ and 0 otherwise. Suppose further that for $t < 0$ the atom is in an initial state $\psi = e^{-i3v} = \cos(3v) - i \sin(3v)$ having momentum $p = -3\hbar k$. The coefficients are most easily obtained by numerical calculation of the Fourier integral.

The amplitude of finding the atom with a momentum +3 at a later time is given by Eq. (26):

$$g_3 = \frac{1}{2} e^{2iqt} \left(\sum_n |A_3^{(2n+1)}|^2 e^{ia_{2n+1}t} + |B_3^{(2n+1)}|^2 e^{ib_{2n+1}t} \right). \quad (28)$$

For the population in the initial state, we find

$$g_{-3}(t) = \frac{1}{2} e^{2iqt} \left(\sum_n |A_3^{(2n+1)}|^2 e^{ia_{2n+1}t} - |B_3^{(2n+1)}|^2 e^{ib_{2n+1}t} \right). \quad (29)$$

I. Losses

The solution (Fig. 1) oscillates quickly around the mean as given by Eq. (27). The frequencies of oscillation are rela-

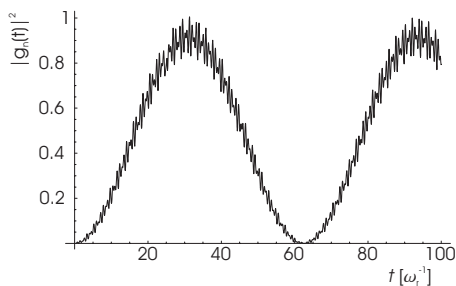


FIG. 1. Population in the final state $|g_n(t)|^2$ as obtained from the Mathieu equation approach plotted versus time t in units of ω_r^{-1} .

tively large compared to the effective Rabi frequency and depend on the pulse amplitudes. Thus, observing them requires very accurate timing and control over the pulse amplitudes. Especially, because of interference fringes in optical setups, it is hard to achieve an amplitude stability better than about 1%. Thus, these oscillations may be hard to observe in practice and the transfer efficiency very close to one at some of their peaks is not useful in practice. Most of the time, the population that can practically be achieved will thus be more close to the mean value as given by Eq. (27). In our previous example, this reaches a maximum of 0.914, i.e., 8.6% of the population are not transferred to the final state.

2. Phase shifts

In this picture, the initial and final momentum states have the same energy. If they were freely propagating (no interactions with neighbor states), their wave function should thus exhibit the same phase factor $\exp(iEt/\hbar)$. The interactions, however, cause a difference of the phase which can be seen by considering the ratio of the amplitudes

$$\tan \phi = \frac{g_{-3}(t)}{g_3(t)}, \quad (30)$$

which can be calculated in a straightforward way. The phase is most conveniently discussed in terms of $\phi - \pi/2$, by subtracting the phase of $\pi/2$ which is expected in the pure Bragg regime, compare Eq. (17). As shown in Fig. 2, this is an oscillating function of time. Around the time for a $\pi/2$ pulse, the amplitude of the oscillation of the relative phase changes are given by $\tan \phi \approx \phi \approx (A_3^{(5)})^2 \approx (B_3^{(5)})^2$. However, since the phase is an oscillatory function, there are instances where the phase is larger or vanishes exactly.

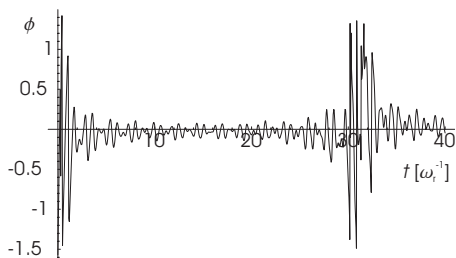


FIG. 2. Phase $\phi - \pi/2$ of the final state relative to the initial state plotted versus time t in units of ω_r^{-1} .

For the practical application of this in atom interferometry, where this relative phase adds to the phase to be measured, two remarks of caution are appropriate: (i) As mentioned before, making use of the theoretically exact vanishing of the phase shift at particular times requires very accurate timing and control over the pulse amplitudes. (ii) In certain interferometer geometries, equal parasitic phases of subsequent beam splitters cancel out. However, since this depends sensitively on very small amplitude changes of the pulses (that would affect the times of the zero crossings of the wiggles in Fig. 2), the cancellation is impaired. Thus, in practice, it may be impossible to rely on this exact vanishing or cancellation.

II. EFFICIENT METHOD FOR CALCULATING THE EFFECTIVE RABI FREQUENCY

The adiabatic elimination process yields a simple equation for the effective Rabi frequency Ω_{eff} . However, it is inappropriate in the quasi-Bragg regime. Higher-order corrections, that tend to reduce Ω_{eff} , will have to be taken into account. In this section, we shall determine these corrections for arbitrary scattering orders. A calculation for second-order scattering has been published previously in [47].

The natural approach to determine Ω_{eff} is via the eigenvalues in the Mathieu equation formalism. This approach can yield Ω_{eff} to any desired accuracy (for constant Ω) by calculating the eigenvalues of the matrix representing an appropriately large subset of the infinite set of equations. In this section, we are looking for an efficient iterative method to calculate Ω_{eff} , for constant as well as time-varying Ω . This is, at the same time, a method for calculating the difference of the eigenvalues $a_m - b_m$ of the Mathieu equation. This method is based on an extension of the idea of adiabatic elimination.

We express the equation of motion, Eq. (12), as the matrix equation

$$\mathcal{H}\vec{g} = i\dot{\vec{g}} \quad (31)$$

where the vector \vec{g} contains the g_n

$$\vec{g} = (\dots, g_{-n}, g_{-n+2}, \dots). \quad (32)$$

In analogy to the above solution in the Mathieu equation formalism, we are interested in a solution that is slowly varying in time, in which the population is mainly consisting of g_{-n} and g_{+n} . The evolution of the other states is governed by the equation

$$\tilde{\mathcal{H}}\tilde{\vec{G}} = \tilde{\vec{c}} + i\dot{\tilde{\vec{G}}}, \quad (33)$$

where $\tilde{\vec{G}}$ is the vector \vec{g} with $g_{\pm n}$ removed, $\tilde{\mathcal{H}}$ is \mathcal{H} with rows and columns of $g_{\pm n}$ removed, and

$$\vec{c} = -\frac{1}{2}(\cdots 0, \Omega g_{-n}, \Omega^* g_{-n}, 0 \cdots 0, \Omega g_{+n}, \Omega^* g_{+n}, 0 \cdots). \quad (34)$$

Suppose for now that $\vec{\mathcal{G}}$ adiabatically follows $g_{\pm n}$, i.e., $i\dot{\vec{\mathcal{G}}} \approx 0$. $\vec{\mathcal{G}}$ thus can be expressed as functions that are linear in \vec{c} , and thus $g_{\pm n}$ (but not necessarily Ω):

$$\vec{\mathcal{G}} = \tilde{\mathcal{H}}^{-1}(\vec{c} + i\dot{\vec{\mathcal{G}}}) \approx \tilde{\mathcal{H}}^{-1}\vec{c} \equiv \vec{\mathcal{G}}^{(0)}. \quad (35)$$

Let us define

$$\vec{\mathcal{G}}^{(0)} \equiv \vec{D}^{(0)}(\Omega, \Omega^*)g_{-n} + \vec{E}^{(0)}(\Omega, \Omega^*)g_{+n}, \quad (36)$$

that is,

$$g_{-n+2m}^{(0)} \equiv D_m^{(0)}(\Omega, \Omega^*)g_{-n} + E_m^{(0)}(\Omega, \Omega^*)g_{+n}. \quad (37)$$

In

$$i\dot{g}_{-n} \approx \frac{\Omega^*}{2}g_{-n-2}^{(0)} + \frac{\Omega}{2}g_{-n+2}^{(0)} \quad (38)$$

we apply Eq. (37) to replace the $g_{-n\pm 2}^{(0)}$ and obtain the analogy to Eq. (16),

$$i\dot{g}_{-n} = \Omega_{\text{ac}}(\Omega, \Omega^*)g_{-n} + \frac{1}{2}\Omega_{\text{eff}}(\Omega, \Omega^*)g_{+n}, \quad (39)$$

where

$$\Omega_{\text{ac}} = \frac{1}{2}(\Omega^* D_{-1}^{(0)} + \Omega D_1^{(0)}), \quad \Omega_{\text{eff}} = \frac{1}{2}(\Omega^* E_{-1}^{(0)} + \Omega E_1^{(0)}). \quad (40)$$

An analogous computation leads to the expansion for g_{+n} ,

$$i\dot{g}_{-n} = \Omega_{\text{ac}}g_{-n} + \frac{\Omega_{\text{eff}}}{2}g_{+n},$$

$$i\dot{g}_{+n} = \Omega_{\text{ac}}g_{+n} + \frac{\Omega_{\text{eff}}^*}{2}g_{-n},$$

in analogy to Eqs. (16), where $|\Omega_{\text{eff}}|$ is the effective Rabi frequency. The leading order in Ω of Ω_{eff} obtained this way is identical to the one obtained in the previous section, see Eq. (15).

Although initially the fast varying $i\dot{\vec{\mathcal{G}}}$ was set to zero by the adiabaticity assumption, we now take into account a slowly varying part due to the adiabatic following, which has similar time scale as the initial and final states and thus cannot be ignored in Eq. (35). In the remainder of this section, $i\dot{\vec{\mathcal{G}}}$ refers to this slowly varying part only. To first order, $i\dot{\vec{\mathcal{G}}}$ can be approximated from $\vec{\mathcal{G}}^{(0)}$:

$$i\dot{\vec{\mathcal{G}}} \approx i\frac{d}{dt}(\vec{\mathcal{G}}^{(0)}). \quad (41)$$

Inserting into Eq. (35),

$$\vec{\mathcal{G}} \approx \vec{\mathcal{G}}^{(0)} + \tilde{\mathcal{H}}^{-1}\left[i\frac{d}{dt}(\vec{\mathcal{G}}^{(0)})\right]. \quad (42)$$

Since $\vec{\mathcal{G}}^{(0)}$ is a function of Ω and $g_{\pm n}$, the time derivatives $i\dot{g}_{\pm n} = \frac{\Omega^*}{2}g_{\pm n-2} + \frac{\Omega}{2}g_{\pm n+2}$ contain $\vec{\mathcal{G}}^{(0)}$ as well as still unknown corrections of $\vec{\mathcal{G}}$. Therefore, care must be taken to properly separate various orders of corrections. We expand $\vec{\mathcal{G}}$ and $i\dot{\vec{\mathcal{G}}}$ as $\vec{\mathcal{G}} = \vec{\mathcal{G}}^{(0)} + \vec{\mathcal{G}}^{(1)} + \cdots$ and $i\dot{\vec{\mathcal{G}}} = \vec{\mathfrak{G}}^{(0)} + \vec{\mathfrak{G}}^{(1)} + \cdots$, where $\vec{\mathcal{G}}^{(l)}$ ($\vec{\mathfrak{G}}^{(l)}$) are an order of magnitude larger than $\vec{\mathcal{G}}^{(l+1)}$ ($\vec{\mathfrak{G}}^{(l+1)}$) and are functions of $g_{\pm n}$ and $\Omega, \dot{\Omega}, \dots$,

$$\vec{\mathcal{G}}^{(l)} = \vec{D}^{(l)}(\Omega, \dot{\Omega}, \dots)g_{-n} + \vec{E}^{(l)}(\Omega, \dot{\Omega}, \dots)g_{+n}. \quad (43)$$

We expand

$$i\dot{\vec{\mathcal{G}}} = \sum_{l,q=0}^{\infty} \left(\frac{\vec{D}^{(l)}}{2}(\Omega^* g_{-n-2}^{(q)} + \Omega g_{-n+2}^{(q)}) + i g_{-n} \dot{\vec{D}}^{(l)} + \frac{\vec{E}^{(l)}}{2}(\Omega^* g_{+n-2}^{(q)} + \Omega g_{+n+2}^{(q)}) + i g_{+n} \dot{\vec{E}}^{(l)} \right),$$

$$i\vec{\mathfrak{G}}^{(p)} = \sum_{l=0}^{l=p} \left(\frac{\vec{D}^{(l)}}{2}(\Omega^* g_{-n-2}^{(q)} + \Omega g_{-n+2}^{(q)}) + i g_{-n} \dot{\vec{D}}^{(l)} + \frac{\vec{E}^{(l)}}{2}(\Omega^* g_{+n-2}^{(q)} + \Omega g_{+n+2}^{(q)}) + i g_{+n} \dot{\vec{E}}^{(l)} \right). \quad (44)$$

Equation (33) thus becomes

$$\tilde{\mathcal{H}} \sum_{p=0}^{\infty} \vec{\mathcal{G}}^{(p)} = \vec{c} + i \sum_{p=0}^{\infty} (i\dot{\vec{\mathcal{G}}})^{(p)} \equiv \vec{c} + i \sum_{p=0}^{\infty} \vec{\mathfrak{G}}^{(p)}. \quad (45)$$

Since the time derivative decreases one order of magnitude for each increase in p , the $(p+1)$ order in Eq. (45) is

$$\tilde{\mathcal{H}}\vec{\mathcal{G}}^{(p+1)} = i\vec{\mathfrak{G}}^{(p)}, \quad \tilde{\mathcal{H}}\vec{\mathcal{G}}^{(0)} = \vec{c}. \quad (46)$$

Thus,

$$\vec{\mathcal{G}}^{(0)} = \tilde{\mathcal{H}}^{-1}\vec{c},$$

$$\vec{\mathcal{G}}^{(p+1)} = i\tilde{\mathcal{H}}^{-1}\vec{\mathfrak{G}}^{(p)} \equiv \vec{D}^{(p+1)}g_{-n} + \vec{E}^{(p+1)}g_{+n}. \quad (47)$$

We are now ready to describe an iterative procedure to obtain $\vec{\mathcal{G}}$ to any desired order: We start from $\vec{\mathcal{G}}^{(0)}$ as defined in Eq. (35). Each component is known as a linear combination of $g_{\pm n}$, and therefore $\vec{D}^{(0)}, \vec{E}^{(0)}$ are also known.

Now suppose that $\vec{\mathcal{G}}^{(q)}, \vec{D}^{(q)}, \vec{E}^{(q)}$ are known for $q \leq p$. In the last equation in Eq. (44), each $g_{-n\pm 2}^{(q)}, g_{+n\pm 2}^{(q)}$ can be expressed as a component of $\vec{\mathcal{G}}^{(q)}$ which, by Eq. (43), is known as a linear combination of $g_{\pm n}$. We insert this into Eq. (47) to obtain $\vec{\mathcal{G}}^{(p+1)}$, again as a linear combination of $g_{\pm n}$. The coefficients of this linear combination are the $\vec{D}^{(p+1)}, \vec{E}^{(p+1)}$. The process can now be iterated to obtain the next higher order.

The efficiency of this method is, in part, due to the fact that each order can be computed using the same inverse matrix $\tilde{\mathcal{H}}^{-1}$. (Moreover, $\tilde{\mathcal{H}}$ is a tridiagonal matrix, which helps in computing the inverse.) Ω_{eff} to M th order is thus obtained by plugging $\sum_{p=0}^M \tilde{\mathcal{G}}^{(p)}$ into Eq. (38) and finding the coefficient of $g_{\pm n}$ as in Eq. (39).

Note that \mathcal{H} and $\tilde{\mathcal{H}}$ in principle are infinite dimensional. However, for obtaining the effective Rabi frequency to order $O(\Omega^{2k})$, it is sufficient to include the initial and final states, states in between, and k nearest neighboring states on each side, i.e., $m = -k, \dots, n+k$. Including more states yields the same result.

With this method, we explicitly calculate the effective Rabi frequency for Bragg diffraction orders of $n \leq 29$. They can be given as power series in Ω and $\dot{\Omega}$,

$$\frac{\Omega_{\text{eff}}}{\omega_r} = \frac{1}{8^{n-1}[(n-1)!]^2} \left(\frac{\Omega}{\omega_r} \right)^n \left| 1 - \sum_{j=1} \alpha_n^{(2j)} \left(\frac{|\Omega|}{\omega_r} \right)^{2j} - \sum_{j=1} \beta_n^{(j)} \left(\frac{\dot{\Omega}}{\omega_r \Omega} \right)^j + \dots \right|. \quad (48)$$

At first, this results in a list of numerical values for the coefficients α and β for each n . However, closed expressions as function of n can be found, which are listed in Appendix A.

Equation (48) also allows us to give validity conditions for the simple adiabatic elimination method presented in Sec. I E 2. For this to be a good approximation, the corrections should be much less than 1. Thus, we obtain

$$\frac{n+2}{2^4(n^2-1)^2} \left(\frac{|\Omega|}{\omega_r} \right)^2 \ll 1, \quad \left| \beta_n^{(1)} \left(\frac{\dot{\Omega}}{\omega_r \Omega} \right) \right| \ll 1. \quad (49)$$

For large n , the first of these conditions translates into $\Omega \ll 4n^{3/2}\omega_r$, which is actually larger than the one given by the adiabaticity condition $\omega_{-n+2m} \geq (n-1)\omega_r \gg \Omega$.

Summing up the population of states other than $g_{\pm n}$ at the end of a pulse (where $g_{-n} \approx 0, g_{+n} \approx 1$), we obtain

$$\vec{\mathcal{G}} \cdot \vec{\mathcal{G}}^* = \frac{n^2+1}{2^5(n^2-1)^2} \left(\frac{|\Omega|}{\omega_r} \right)^2 + \frac{(n^4+6n^2+1)}{2^9(n^2-1)^4} \left| \left(\frac{\dot{\Omega}}{\omega_r^2} \right) \right|^2 + \dots \quad (50)$$

The population lost into other states after the pulse is switched off, when $\Omega = \dot{\Omega} = 0$, vanishes. The method presented in this section is not suitable for obtaining those losses, because the states other than $g_{\pm n}$ have been assumed to adiabatically follow their neighbors, and the losses are a nonadiabatic phenomenon.

However, as long as $|g_{m \neq \pm n}|^2 \ll |g_{\pm n}|^2$, the effect of the losses on $g_{\pm n}$ and thus Ω_{eff} can be neglected.

This iterative method, although powerful for calculating Ω_{eff} , does not approach an exact solution. It can be seen from Eq. (39) that this method gives no wiggles in the sinusoidal change of the initial- or final-state population, while there are fast variations in the exact solution of a square pulse as shown in Mathieu function section. However, it approaches the solution for the initial and final state as averaged over the

high-frequency wiggles, Eq. (27) and thus predicts the correct effective Rabi frequency.

III. ADIABATIC EXPANSION

To investigate the losses, corrections to the adiabatic method must be calculated. We will relabel the results $g_{\pm n}$ of the adiabatic method as $g_{\pm n}^{(1)}$. They represent the first-order adiabatic approximation. We now want to calculate corrections to the population of the states,

$$g_m = g_m^{(1)} + g_m^{(2)} + \dots, \quad (51)$$

where to first order only the initial and final state are nonzero. For calculating the second order, we insert $g_{\pm n}^{(1)}$ into Eqs. (12). Inserting $g_{\pm n}^{(1)}$ from Eq. (17), we obtain population of the levels next to the initial and final states to second order

$$\begin{aligned} i\dot{g}_{-n\pm 2} &= 4(1 \mp n)\omega_r g_{-n\pm 2} + \frac{1}{2}\Omega \cos\left(\frac{1}{2}\int_{-\infty}^t \Omega_{\text{eff}}(t') dt'\right), \\ i\dot{g}_{n\pm 2} &= 4(1 \pm n)\omega_r g_{n\pm 2} - \frac{i}{2}\Omega \sin\left(\frac{1}{2}\int_{-\infty}^t \Omega_{\text{eff}}(t') dt'\right), \end{aligned} \quad (52)$$

where $n > 2$. These are all states for which $g^{(2)} \neq 0$. The process can be iterated: From the $g_{\pm n\pm 2}^{(2)}$, corrections $g^{(3)}$ can be obtained, and so forth. Here and throughout, we shall drop the superscript 2 as long as no confusion arises.

These inhomogenous equations can be solved by standard methods, such as variation of the constant or a Green's function,

$$\begin{aligned} g_{-n\pm 2}(t) &= -\frac{i}{2}\int_{-\infty}^t dt_0 \Omega(t_0) \cos\left(\frac{1}{2}\int_{-\infty}^{t_0} \Omega_{\text{eff}}(t') dt'\right) \\ &\quad \times e^{-4i(1 \mp n)\omega_r(t-t_0)} \theta(t-t_0), \\ g_{n\pm 2}(t) &= -\frac{1}{2}\int_{-\infty}^t dt_0 \Omega(t_0) \sin\left(\frac{1}{2}\int_{-\infty}^{t_0} \Omega_{\text{eff}}(t') dt'\right) \\ &\quad \times e^{-4i(1 \pm n)\omega_r(t-t_0)} \theta(t-t_0). \end{aligned} \quad (53)$$

A. Losses

We are mainly interested in the population $g_n \equiv g_n(\infty)$. For that, we can take out a phase factor and note that $\theta(t-t_0) = 1$. The absolute squares of these give the population in the neighboring states. These are closed, analytic expressions for the losses arising in the second order. As an example for a third-order correction,

$$\begin{aligned} g_{-n-4}^{(3)}(t) &= -\frac{i}{2}\int_{-\infty}^t dt_3 \Omega(t_3) e^{-8i(2+n)\omega_r(t-t_3)} \theta(t-t_3) \\ &\quad \times \left(-\frac{i}{2}\right) \int_{-\infty}^{t_3} dt_2 \Omega(t_2) e^{-4i(1+n)\omega_r(t_3-t_2)} \\ &\quad \times \theta(t_3-t_2) \cos\left(\frac{1}{2}\int_{-\infty}^{t_2} \Omega_{\text{eff}}(t_1) dt_1\right). \end{aligned} \quad (54)$$

B. Phase shifts

To third order, both $g_{n\pm 2}^{(2)}$ contribute to $g_n^{(3)}$,

$$g_n^{(3)} = \frac{-1}{4} \int_{-\infty}^t dt_3 \Omega(t_3) \int_{-\infty}^{t_3} dt_2 \Omega(t_2) \times [e^{-4i(1-n)\omega_r(t_3-t_2)} + e^{-4i(1+n)\omega_r(t_3-t_2)}] \times \cos\left(\frac{1}{2} \int_{-\infty}^{t_2} \Omega_{\text{eff}}(t_1) dt_1\right). \quad (55)$$

[The $\theta(t_3-t_2)$ has been omitted because it is one throughout the t_2 integration range.] Since this is a complex number, the phase of $g_n^{(1)} + g_n^{(3)}$ will be shifted by some $\Delta\phi$ relative to the adiabatic result, $g_n^{(1)}$.

An upper limit on $\Delta\phi$ can be derived as follows: We will assume that all the losses derived in the previous section in second order contribute to 100% to $g_n^{(3)}$. Furthermore, we will assume that the phase of these contributions is 90° shifted relative to $g_n^{(1)}$. This will result in an upper limit on $\Delta\phi$, since in reality only a fraction of the losses in second order will be reintroduced into the final state to third order, and since a 90° phase of these contributions is the worst case. Then,

$$|\Delta\phi| \leq \frac{|g_n^{(3)}|}{|g_n^{(1)} + g_n^{(3)}|} \approx |g_n^{(3)}| \leq \sqrt{\ell}, \quad (56)$$

where the total losses are denoted ℓ .

The equations derived in this chapter are closed expressions for the calculation of losses and phase shifts for realistic, time-dependent envelope functions. We will apply them to square and Gaussian pulses in the next two chapters.

IV. SQUARE PULSES

These expressions for the second order are easily solved for square pulses having a peak two-photon Rabi frequency of $\bar{\Omega}$ for $0 < t < T$ and zero otherwise. For the effective Rabi frequency, we can use the result from the simple adiabatic elimination method, because, as it will turn out, losses become very large already in the region where this is still valid. In this case,

$$g_{-n\pm 2} = -i \frac{\bar{\Omega}}{2} \int_0^T dt_0 \cos\left(\frac{\pi t_0}{2T}\right) e^{4i(1\mp n)\omega_r t_0},$$

$$g_{n\pm 2} = -\frac{\bar{\Omega}}{2} \int_0^T dt_0 \sin\left(\frac{\pi t_0}{2T}\right) e^{4i(1\pm n)\omega_r t_0}. \quad (57)$$

The integrals can be calculated in a straightforward way; the result can be simplified by considering the terms linear in $\bar{\Omega}$ only [noting that $(\omega_r T)^{-1}$ is proportional to $\bar{\Omega}^n/\omega_r^n$]. This does not lead to reduced accuracy, since in this second-order adiabatic expansion, terms of higher order can be assumed to be zero. We obtain

$$g_{-n\pm 2} = \frac{\bar{\Omega}}{\omega_r} \frac{1}{8(1\mp n)},$$

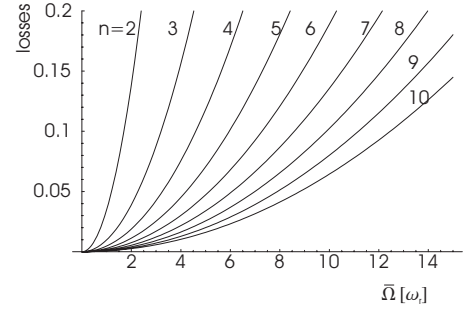


FIG. 3. Losses for square pulses for $n=2, \dots, 10$, plotted versus $\bar{\Omega}/\omega_r$.

$$g_{n\pm 2} = i \frac{\bar{\Omega}}{\omega_r} \frac{1}{8(1\pm n)} e^{4i(1\pm n)\omega_r T}. \quad (58)$$

The losses in the final and initial state are $\ell = |g_{-n-2}|^2 + |g_{-n+2}|^2 + |g_{n-2}|^2 + |g_{n+2}|^2 = 2(|g_{n-2}|^2 + |g_{n+2}|^2)$. We obtain

$$\ell = \frac{1}{16} \frac{\bar{\Omega}^2}{\omega_r^2} \frac{n^2 + 1}{(n^2 - 1)^2}, \quad (59)$$

as plotted in Fig. 3. As an example, for $n=3, \bar{\Omega}=3$ we have $\ell=0.088$, in excellent agreement with the exact solution in terms of Mathieu functions (0.086).

The square root of this is at the same time an upper limit on the phase shift for a $\pi/2$ pulse, and indeed the exact solution as plotted in Fig. 2 verifies this. Square pulses are thus, unfortunately, not suitable for quasi-Bragg scattering, because $\bar{\Omega}$ must be reduced strongly if low losses and phase shifts are desirable. Already the above example, with 9% losses and thus ~ 0.3 rad maximum phase requires a π -pulse time of about $30/\omega_r$, or about 3 ms for cesium atoms. Reduction of this to below 10^{-4} , as required for high-precision atom interferometers, would take a pulse time of about 10^6 seconds.

In the next chapter, we will study pulses with a smooth envelope function, Gaussian pulses. These will exhibit much lower losses and phase shifts for a given pulse duration.

V. GAUSSIAN PULSES

In this section, we specialize to Gaussian pulses,

$$\Omega = \bar{\Omega} e^{-t^2/(2\sigma^2)}, \quad (60)$$

so that, from Eq. (15),

$$\Omega_{\text{eff}} = \bar{\Omega}^n \left(\frac{1}{8\omega_r}\right)^{n-1} \frac{1}{[(n-1)!]^2} e^{-t^2 n/(2\sigma^2)}. \quad (61)$$

The case of Gaussian pulses is more difficult. (i) One the one hand, this is because the integrals are much harder. (ii) With Gaussian pulses, higher Rabi frequencies can be used. Thus, we need to take into account higher-order corrections for the effective Rabi frequency.

For now specializing to π pulses, we have the condition

$$\frac{1}{2} \int_{-\infty}^{\infty} \Omega_{\text{eff}}(t') dt' = \frac{\bar{\Omega}^n}{2} \left(\frac{1}{8\omega_r} \right)^{n-1} \frac{\sqrt{2\pi\sigma^2}}{[(n-1)!]^2 \sqrt{n}} = \frac{\pi}{2}, \quad (62)$$

that we will use to determine σ . We insert into the expressions for the amplitudes of the neighbor states and obtain

$$g_{-n\pm 2} = -i \frac{\bar{\Omega}}{2} \int_{-\infty}^{\infty} dt e^{-t^2/(2\sigma^2)} \cos \left[\frac{\pi}{4} \text{erf} \left(\sqrt{\frac{n}{2\sigma^2}} t \right) \right] e^{4i(1\mp n)\omega_r t}, \quad (63)$$

$$g_{n\pm 2} = -\frac{\bar{\Omega}}{2} \int_{-\infty}^{\infty} dt e^{-t^2/(2\sigma^2)} \sin \left[\frac{\pi}{4} \text{erf} \left(\sqrt{\frac{n}{2\sigma^2}} t \right) \right] e^{4i(1\pm n)\omega_r t}. \quad (64)$$

We denoted $\text{erf}(x) = 1 + \Phi(x)$ and Φ is the error function

$$\Phi(x) \equiv \frac{2}{\sqrt{\pi}} \int_0^x e^{-t^2} dt. \quad (65)$$

For $\pi/2$ pulses, the factors of $\pi/4$ in the last three equations will be replaced by $\pi/8$. No simpler form of this integrals has been found. However, for π pulses, we can use

$$\sin \left(\frac{\pi}{4} + x \right) = \frac{\cos x + \sin x}{\sqrt{2}} = \cos \left(\frac{\pi}{4} - x \right) \quad (66)$$

and $\Phi(x) = -\Phi(-x)$ to obtain $g_{-n\pm 2} = i g_{n\mp 2}^*$.

Inclusion of higher-order corrections to the effective Rabi frequency. For Gaussian pulses, the peak effective Rabi frequency can reach a level beyond the region of validity of Eq. (15) before the losses as predicted from the results of the last section become noticeable. In this region, however, the second-order adiabatic solution is still a good approximation, as long as the losses it predicts are still low (because then, the third order will be even lower). Therefore, we can extend the region of validity into the interesting region, where the losses just start, by including higher-order corrections to Ω_{eff} as calculated in Sec. II. In principle, of course, adiabatic expansion to higher and higher orders is a systematic way of obtaining results of similar and higher accuracy and simultaneously predict the changes in the effective Rabi frequency. However, this is very inconvenient method for Gaussian pulses, for which the integral is hard even in the second order.

For a π pulse we have the condition

$$\frac{1}{2} \int_{-\infty}^{\infty} \Omega_{\text{eff}}(t') dt' = \frac{\pi}{2}. \quad (67)$$

We insert Eq. (48) and note that while the α coefficients and $\beta_n^{(2)}$ are real, $\beta_n^{(1)}$ is imaginary. Ω_{eff} is given by the absolute magnitude of the series and we expand the absolute value as a Taylor series in terms of the imaginary part that we truncate after the $(\dot{\Omega})^2$ terms.

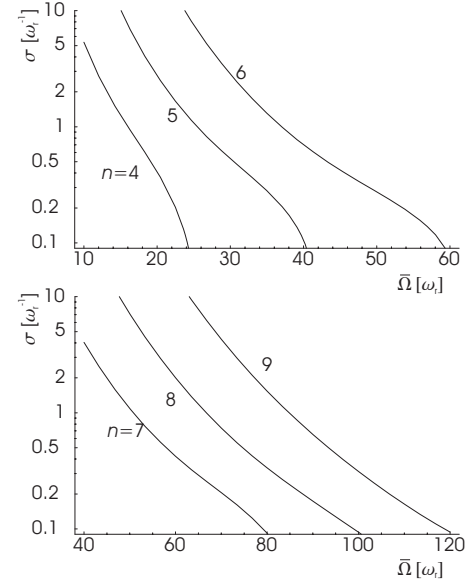


FIG. 4. σ in units of ω_r for π pulses for Bragg diffractions of order $n=4,5,6$ (above) and $n=7,8,9$ (below) plotted versus $\bar{\Omega}$. The effective Rabi frequency has been inserted up to order $\bar{\Omega}^{n+6}$.

$$\frac{\Omega_{\text{eff}}}{\omega_r} \approx \frac{1}{8^{n-1} [(n-1)!]^2} \left(\frac{\Omega}{\omega_r} \right)^n \left[1 - \sum_{j=1}^{n-1} \alpha_n^{(2j)} \left(\frac{|\dot{\Omega}|}{\omega_r} \right)^{2j} - \tilde{\beta} \left(\frac{\dot{\Omega}}{\omega_r \Omega} \right)^2 \right], \quad (68)$$

where

$$\tilde{\beta} = -\frac{1}{2} |\beta_n^{(1)}|^2 + \beta_n^{(2)}. \quad (69)$$

This approximation will be justified in retrospect, as we will find that transitions having low loss satisfy the condition equation (74), which gives a lower limit on σ [53]. At this limit, the leading neglected terms ($\beta_n^{(3)}$ and $\tilde{\beta} \alpha_n^{(2)}$) are starting to become non-negligible and the comparison to a numerical simulation shows an about 10% error in the predicted sigma, see Sec. V D. The inclusion of more terms would reduce the error here, but would lead to extremely lengthy expressions later. In the region of low loss, they are negligible.

The condition for a π pulse reads

$$\begin{aligned} \frac{\bar{\Omega}^n}{2} \left(\frac{1}{8\omega_r} \right)^{n-1} \frac{\sqrt{2\pi\sigma^2}}{[(n-1)!]^2 \sqrt{n}} & \left(1 - \tilde{\beta} \frac{1}{n\omega_r^2 \sigma^2} - \dots \right. \\ & - \alpha_n^{(2)} \frac{\bar{\Omega}^2}{\omega_r^2} \sqrt{\frac{n}{n+2}} - \alpha_n^{(4)} \frac{\bar{\Omega}^4}{\omega_r^4} \sqrt{\frac{n}{n+4}} - \alpha_n^{(6)} \frac{\bar{\Omega}^6}{\omega_r^6} \sqrt{\frac{n}{n+6}} \\ & \left. - \dots \right) = \frac{\pi}{2}. \end{aligned} \quad (70)$$

From this, σ can be computed without difficulty, see Fig. 4. In the following, we take into account the higher-order corrections up to order $\bar{\Omega}^{n+6}$ and $1/(\omega_r \sigma)^2$. For the integrals

appearing in the trigonometric functions, we find

$$\begin{aligned} \frac{1}{2} \int_{-\infty}^t \Omega_{\text{eff}}(t') dt' &= \frac{\bar{\Omega}^n}{(8\omega_r)^{n-1} [(n-1)!]^2} \sqrt{\frac{\pi\sigma^2}{2n}} \\ &\times \left[\left(1 - \bar{\beta} \frac{1}{n\omega_r^2\sigma^2} \right) \text{erf} \left(\sqrt{\frac{n}{2}} \frac{t}{\sigma} \right) \right. \\ &\left. - \sqrt{\frac{n}{n+2}} \alpha_n^{(2)} \frac{\bar{\Omega}^2}{\omega_r^2} \text{erf} \left(\sqrt{\frac{n+2}{2}} \frac{t}{\sigma} \right) \right] \end{aligned}$$

$$\begin{aligned} &- \sqrt{\frac{n}{n+4}} \alpha_n^{(4)} \frac{\bar{\Omega}^4}{\omega_r^4} \text{erf} \left(\sqrt{\frac{n+4}{2}} \frac{t}{\sigma} \right) \\ &- \frac{\bar{\beta}}{\omega_r^2\sigma^3} \sqrt{\frac{2}{n\pi}} t e^{-n^2/2\sigma^2} \left. \right]. \quad (71) \end{aligned}$$

Making the same assumptions as above, we can neglect the $1/\sigma^3$ term. Using Eq. (71), we can write

$$\begin{aligned} &\sin \left(\frac{1}{2} \int_{-\infty}^t \Omega_{\text{eff}}(t') dt' \right) \\ &= \sin \left(\frac{\pi}{4} \frac{\left(1 - \bar{\beta} \frac{1}{2n\omega_r^2\sigma^2} \right) \text{erf} \left(\sqrt{\frac{n}{2}} \frac{t}{\sigma} \right) - \sqrt{\frac{n}{n+2}} \alpha_n^{(2)} \frac{\bar{\Omega}^2}{\omega_r^2} \text{erf} \left(\sqrt{\frac{n+2}{2}} \frac{t}{\sigma} \right) - \sqrt{\frac{n}{n+4}} \alpha_n^{(4)} \frac{\bar{\Omega}^4}{\omega_r^4} \text{erf} \left(\sqrt{\frac{n+4}{2}} \frac{t}{\sigma} \right)}{1 - \bar{\beta} \frac{1}{n\omega_r^2\sigma^2} - \alpha_n^{(2)} \frac{\bar{\Omega}^2}{\omega_r^2} \sqrt{\frac{n}{n+2}} - \alpha_n^{(4)} \frac{\bar{\Omega}^4}{\omega_r^4} \sqrt{\frac{n}{n+4}}} \right). \end{aligned}$$

The functions $\text{erf}(\sqrt{n/2}t)$, $\text{erf}(\sqrt{(n+2)/2}t)$, ..., although similar, show an increasing slope with respect to t . As they are integrated over, and as $\sqrt{(n+2)/2} \approx \sqrt{n/2}$, this is insignificant for large n and we can take these functions to be equal. We then recover Eq. (63), the only difference being the replacement of σ by the solution of Eq. (70). It remains to actually calculate the integral.

This integral is a function of n and σ . σ , in turn, is determined by $\bar{\Omega}$ for π or $\pi/2$ pulses. Unfortunately, the integral cannot be solved exactly. The general structure of the integrand is a periodic oscillating function $\exp[-i\omega_r(1 \pm n)t]$ times an envelope that is peaked near $t=0$. For $g_{n \pm 2}$, the peak is limited on the right mainly by the Gaussian $\exp[-t^2/(2\sigma^2)]$ and on the left by the sine of the error function. For low Rabi frequencies, σ is high and thus the peak is broad compared to the period $1/[(n \pm 1)\omega_r]$ of the oscillating function, which thus averages out to a very low value. When the peak width becomes comparable to the period, however, this is no longer the case and the value of the integral will increase. Since we are interested in the region where the losses are nonzero, but still low, it is sufficient to solve the integral with a method that is valid in this region. The method of steepest descent, or ‘‘saddle-point’’ method is suitable. As derived in Appendix C, neglecting a phase factor that is of no consequence unless one wants to proceed to higher orders,

$$g_{n \pm 2} = -\bar{\Omega} D \sqrt{2\sigma^2} \exp \left\{ -8(1 \pm n)^2 \frac{\sigma^2 \omega_r^2}{n^{1/3} \Gamma} \right\} = i g_{-n \mp 2}^*, \quad (72)$$

see Eq. (C10). Here, $\Gamma \approx 1.64874$ and D is a factor of the order one that is given in Eq. (C12) and plotted in Fig. 10.

Alternatively, the integral can be computed numerically, see Fig. 5. Accurate numerical computation, however, becomes difficult when the losses are low, because then the integrand will make very many oscillations. The saddle-point method, however, works well especially in this region. Comparison of both shows good agreement for the range we are interested in, where the losses are lower than about 10%.

As shown in Appendix C, the results can be easily adapted to $\pi/2$ pulses if Γ is replaced by $\Gamma_{\pi/2} = 1.5043$ and D by $D_{\pi/2}$, which is also plotted in Fig. 10. Thus, the losses for π and $\pi/2$ pulses are essentially the same.

A. Losses

The losses in the final and initial state are $\ell = |g_{-n-2}|^2 + |g_{-n+2}|^2 + |g_{n-2}|^2 + |g_{n+2}|^2 = 2(|g_{n-2}|^2 + |g_{n+2}|^2)$. Since the terms

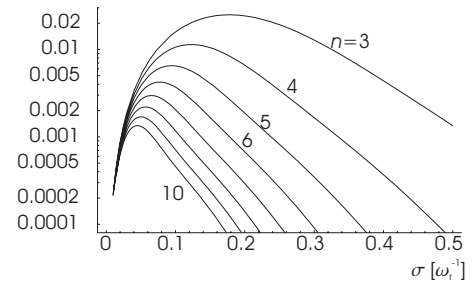


FIG. 5. Numerical calculation of the integral $\int_{-\infty}^{\infty} \exp[-t^2/(2\sigma^2) - i\omega_r(1-n)t] \text{erf} \left\{ (\pi/4) \sin \left[\sqrt{n/2} (t/\sigma) \right] \right\} dt$ as plotted versus σ . Parameter: $n=3, 4, \dots, 10$. σ is in units of inverse recoil frequencies.

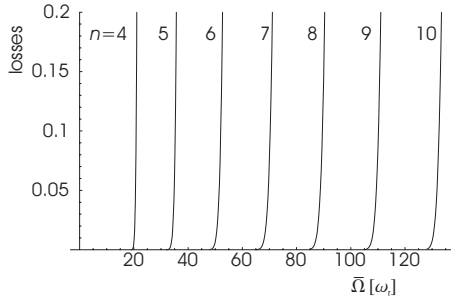


FIG. 6. Losses for Gaussian π pulses for Bragg diffractions of order $n=4$ to 10 plotted versus $\bar{\Omega}$. The effective Rabi frequency has been inserted up to order $\bar{\Omega}^{n+6}$.

with the plus sign in the exponential can be neglected, we obtain a simple form

$$\ell = 4(\bar{\Omega}D\sigma)^2 e^{-16(1-n)^2\sigma^2\omega_r^2/(n^{1/3}\Gamma)}. \quad (73)$$

For losses below the 10^{-2} level, we have the condition (the factors outside the exponential are of order one)

$$\sigma\omega_r > \frac{\sqrt{2\Gamma \ln(2)n^{1/6}}}{4(n-1)} \approx 0.38 \frac{n^{1/6}}{n-1}. \quad (74)$$

Since the losses decrease rapidly with longer σ , very low losses can be reached: For example, if the theoretical losses should be lower than 10^{-10} (which is then clearly negligible compared to losses due to technical influences),

$$\sigma\omega_r > 1.5 \frac{n^{1/6}}{n-1}. \quad (75)$$

We can now compute the losses and pulse durations as functions of $\bar{\Omega}$, see Figs. 6 and 4.

B. Phase shifts

As discussed, the parasitic phase shifts in radians are at most equal to the square root of the losses, as computed in the previous section. Since the losses are such a steep function of $\bar{\Omega}$, slightly reducing $\bar{\Omega}$ below the level where the losses become appreciable will essentially reduce the phase shifts to negligible levels. For example, if Eq. (75) is satisfied, these theoretical shifts will be below 10^{-5} .

For Gaussian pulses with an appropriate choice of $\bar{\Omega}$, the theoretical losses considered here are so low that they are negligible in practice. The practical losses will then be dominated by issues such as single-photon excitation, finite laser beam size, finite size and temperature of the atomic cloud, wave-front distortions, and other things. These losses are based on entirely different mechanisms and will therefore not necessarily lead to a phase shift as the theoretical losses calculated in this paper.

C. Truncated Gaussians

Any experimental realization of the Gaussian must be truncated somewhere. Here, we consider the modifications of

the above considerations that arise if the Gaussian is truncated on the right side (only) at $t=\tau \gg \sigma$. The integrations in Eq. (63) will now run from $-\infty$ to τ . It is convenient to write the final state after a truncated Gaussian pulse as $g_{-n\pm 2, n\pm 2} + g_{-n\pm 2, n\pm 2}^\tau$, where $g_{-n\pm 2, n\pm 2}$ is given by Eq. (63) and

$$g_{-n\pm 2}^\tau = i \frac{\bar{\Omega}}{2} \int_\tau^\infty dt e^{-t^2/(2\sigma^2)} \cos\left\{ \frac{\pi}{4} \operatorname{erf}\left(\sqrt{\frac{n}{2\sigma^2}} t \right) \right\} e^{4i(1\mp n)\omega_r t}, \quad (76)$$

$$g_{n\pm 2}^\tau = \frac{\bar{\Omega}}{2} \int_\tau^\infty dt e^{-t^2/(2\sigma^2)} \sin\left\{ \frac{\pi}{4} \operatorname{erf}\left(\sqrt{\frac{n}{2\sigma^2}} t \right) \right\} e^{4i(1\pm n)\omega_r t}. \quad (77)$$

Since $\tau \gg \sigma$, we can use $\Phi(t) \approx 1 - e^{-t^2}/(\sqrt{\pi}t)$ and approximate the trigonometric functions to leading order of the argument. We obtain

$$g_{-n\pm 2}^\tau = i \frac{\bar{\Omega}}{8} \sqrt{\frac{2\pi\sigma^2}{n}} \int_\tau^\infty \frac{dt}{t} e^{-(n+1)t^2/(2\sigma^2) + 4i(1\mp n)\omega_r t},$$

$$g_{n\pm 2}^\tau = -\frac{\bar{\Omega}}{2} \int_\tau^\infty dt e^{-t^2/(2\sigma^2)} e^{4i(1\pm n)\omega_r t}. \quad (78)$$

For $t \gg \tau \gg \sigma$, the Gaussian $e^{-t^2/(2\sigma^2)}$ (and *a fortiori* $e^{-(n+1)t^2/(2\sigma^2)}$) is a very steep function of t , which is non-negligible only in a small region above τ . In fact, we can assume that the other functions in the integral are constant and have the values they take at $t=\tau$. The integrals then reduce to error functions, which in turn can be replaced by the asymptotic expression for large arguments. We obtain

$$g_{-n\pm 2}^\tau = -i \frac{\bar{\Omega}}{4} \frac{\sigma^3}{\sqrt{n(n+1)}\tau^2} e^{-(n+1)\tau^2/(2\sigma^2)} e^{4i(1\mp n)\omega_r \tau},$$

$$g_{n\pm 2}^\tau = \frac{\bar{\Omega}\sigma^2}{\sqrt{\pi}\tau} e^{-\tau^2/(2\sigma^2)} e^{4i(1\pm n)\omega_r \tau}. \quad (79)$$

Truncation on the left interchanges the expressions for $g_{n\pm 2}^\tau$ and $g_{-n\pm 2}^\tau$.

For an example, consider $\tau = \sigma\sqrt{-2 \ln(\eta)}$ is chosen such that the truncation happens at a fraction η of the peak amplitude. Obviously, the smaller η , the smaller the effect of truncation, which also decreases for large n (as expected, as the Gaussian to the power of n has a narrower peak). Consider, for example, $\eta = 1/100$ (i.e., $\tau \approx 3\sigma$) and $n=5$. Then, $|g_{-n\pm 2}^\tau| = 3.9 \times 10^{-15} \bar{\Omega}\sigma$. That means, the effects of truncation can be reduced to negligible magnitude.

In order to keep phase shifts low, it is desirable to choose τ such that $4\omega_r\tau = 2\pi, 4\pi, \dots$, in which case the amplitudes for the neighbor states are real, i.e., there is no extra phase shift due to the truncation. On the other hand, purposely truncating the pulses at a variable τ thus provides a means of testing the influence of these phase shifts in experiments.

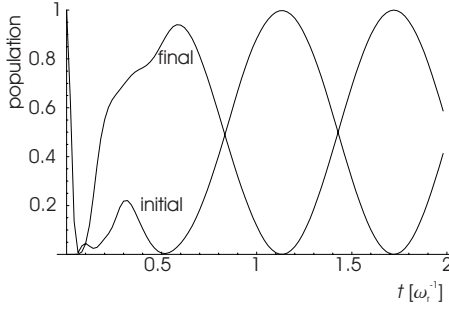


FIG. 7. Simulated populations of the initial and final state for $n=5$, $\bar{\Omega}=38$ plotted versus σ in units of inverse recoil frequencies.

D. Accuracy of the estimates and higher-order effects

The losses are very steep functions of $\bar{\Omega}$. Therefore, the error in the predicted loss for a given Rabi frequency is much larger than the error in the inverse function, the Rabi frequency for a given loss. To confirm these results, we numerically integrate the Schrödinger equation in the momentum representation. We include sufficiently many “outer” momentum states until the results are essentially unaffected by including more (usually, 5 are sufficient). The simulation program itself is checked for constant Rabi frequency against the exact solution in terms of Mathieu functions.

The result for Gaussian pulses with $n=5$ and $\bar{\Omega}=38\omega_r$ is shown in Fig. 7. For $\sigma \leq 0.1/\omega_r$, most of the population is still left in the initial state, $|g_{-5}|^2 \approx 1$. For slightly larger σ , the population is driven out of the initial state. However, the transfer efficiency to the final state g_5 is very low, as expected in the Raman-Nath regime. When the pulse becomes longer, the system enters the quasi-Bragg regime and the losses become quite low. At $\sigma=0.52/\omega_r$, the population of the initial state has a minimum of $|g_{-5}|^2 \approx 0.0035$, whereas the population of the final state $|g_5|^2 \approx 0.89$. The remaining 11% of the population are lost into other states. At $\sigma \approx 0.58/\omega_r$, the final state has a first maximum of $|g_5|^2 \approx 0.94$; at this time, $|g_{-5}|^2 \approx 0.029$, i.e., about 6% are lost into other orders. Thus, in this regime, the minimum of the initial and the maximum of the final state do not coincide. For even larger σ , the losses become negligible and the system performs Pendellösung oscillations just as in the Bragg regime, although the adiabaticity criterion is still violated.

For comparison, the second-order adiabatic theory predicts about 6% losses for $\bar{\Omega}=36$, rather than 38. The bulk of the 15% discrepancy is due to the remaining error in the calculation of σ from Eq. (70). Another prediction of the theory that is confirmed by the simulation is the symmetry of the losses $g_{n\pm 2} = -g_{-n\mp 2}$.

To third order, a part of the population that is lost to the neighbor states to second order returns to the initial and final state in the third order. This has two main effects: First, it reduces the predicted losses. Second, since the returning population will have a different time dependence for the initial and final state, it can account for the difference of the σ that gives maximum population in the final state versus the one that gives a minimum in the initial state. We will not consider this.

E. Practical example

Suppose we want to achieve $2n=16$ photon Bragg diffraction with the lowest possible time compatible with losses below 1%. Equation (74) gives a minimum $\sigma \geq 0.08\omega_r^{-1} \approx 6 \mu\text{s}$. This is substantially faster than allowed by the adiabaticity limit equation (19), which would require $\Omega_{\text{eff}} \ll 0.007\omega_r \approx 2\pi \times 14 \text{ Hz}$, i.e., transition times on the order of 0.1 s. For applications in precision atom interferometry, where the unwanted phase shift, that is estimated as the square root of the losses, must be low, we might want to have theoretical losses as low as 10^{-10} (even if then additional losses due to technical reasons will be much larger). This can be obtained with $\sigma \geq 0.3\omega_r^{-1} \approx 24 \mu\text{s}$, according to Eq. (75). For this case, we can read off a required peak two-photon Rabi frequencies of $\bar{\Omega} \sim 80\omega_r$ from Fig. 4.

For an explicit example, consider cesium atoms driven on the $6^2S_{1/2}$, $F=4$, $m_F=0 \rightarrow 6^2P_{3/2}$ (D2) transition which has a wavelength of 852 nm, with a detuning of 10 GHz. The relevant data of that transition is found in Ref. [54]. To determine the two-photon Rabi frequency, we neglect the hyperfine splitting of the excited state (which is on the order of a few 100 MHz) and sum over the excited states $|F'=5, m_F=1\rangle$, $|F'=4, m_F=1\rangle$, and $|F'=3, m_F=1\rangle$. From summing the matrix elements, we obtain a two-photon Rabi frequency of $\bar{\Omega} = \frac{2}{3}(I/I_{\text{sat}})^{\frac{1}{4}}(\Gamma^2/\delta)$, or $\bar{\Omega}/\omega_r = 0.20I/(\text{mW}/\text{cm}^2)$, where $I_{\text{sat}} = 1.1 \text{ mW}/\text{cm}^2$.

If we have, for example, laser beams with a Gaussian waist of $w_0=0.6 \text{ cm}$, the intensity at the center is $I = 2P/(\pi w_0^2)$, where P is the total power. Inserting, we obtain $\bar{\Omega}/\omega_r = 0.35P/\text{mW}$. Thus, a power of about 250 mW is necessary to reach $\bar{\Omega}/\omega_r \approx 88$.

VI. DISCUSSION, SUMMARY, AND OUTLOOK

We have given an analytic theory of quasi-Bragg scattering. This is the range of short-interaction times for which the usual adiabatic theory of Bragg scattering breaks down. Thus, population shows up in scattering orders other than those allowed by the Bragg condition. However, we find that this population can still be extremely low provided that the interaction is switched on and off with a smooth envelope function.

For calculating these effects, we introduced a method for solving the Schrödinger equation, adiabatic expansion. The Schrödinger equation in momentum space is a coupled system of differential equations describing the population in the different momentum states. A first approximate solution is obtained in the usual way by adiabatically eliminating the states between the initial and the final state. We then reinsert this first-order solution into the Schrödinger equation. This results in inhomogenous differential equations for the momentum states next to the initial and final state. Thus, we obtain a second-order solution. While this process can be iterated, the second order is sufficient for our purposes. Unlike previous approaches, this method allows us to treat arbitrary diffraction orders and envelope functions. We expect that this method is useful for obtaining higher accuracy re-

sults in all situations that are usually treated by adiabatic elimination.

We also present an efficient method for calculating the effective Rabi frequency, which is related to the eigenvalues of Mathieu functions. Closed expressions are obtained for the Rabi frequency up to eighth-order corrections for arbitrary Bragg diffraction order.

We treat diffraction with a scatterer having square and Gaussian envelope functions as examples. Square envelopes lead to a high loss of the population into undesired momentum states (as experimentally observed, e.g., by [1]). Moreover, due to couplings of the desired output state with the loss channels, the output state becomes phase shifted as a function of the interaction strength and duration. On the other hand, Gaussian envelopes can lead to extremely low losses, and hence phase shifts, even for pulse times that substantially violate the adiabaticity criterion. The effects of truncation of the Gaussian to a finite wave form can be made negligible by suitably chosen truncation. Comparison to a numerical integration of the Schrödinger equation verifies that the second order is sufficient for our purposes.

While these results are important in all situations where Bragg diffraction is applied (such as acousto-optic modulators), we focus on the context of atom interferometry. For example, some present high-precision atom interferometers demand phase errors $\Delta\phi$ below 10^{-5} rad [35]. For Gaussian pulses, the total losses ℓ are given by Eq. (73) and $\Delta\phi \sim \sqrt{\ell} \leq 10^{-5}$ can be satisfied by operating with a σ longer than about $1.5/\omega_r$, see Eq. (75). The strong dependence of ℓ on $\bar{\Omega}$ means that a slight reduction of $\bar{\Omega}$ corresponds to a strong reduction of $\Delta\phi$. On the other hand, for square pulses, $\sqrt{\ell} \leq 10^{-5}$ can only be fulfilled for $\bar{\Omega} \ll \omega_r$, which will in practice mean unrealistically long transition times.

While atom interferometry is a field to which our calculations are, we hope, useful, in this work we restricted attention to one single beam splitter. The application of the results to a full interferometer, e.g., in the Ramsey-Bordé or other geometries, is a matter that we did not consider. While we considered the phase shift arising within one beam splitter, the signal of an atom interferometer is given by the total amplitude of all interfering momentum states. In certain situations, the neighboring momentum states (considered as “losses” in here) contribute to this, leading to an apparent distortion of the interference fringes. This has been considered for the Raman-Nath regime in [55,56]. An upper limit for this can be given by $\sqrt{\ell}$, by assuming that all the lost population interferes and conspires to produce the maximum effect. Thus, operation in the quasi-Bragg regime is suitable for reducing this contribution. Moreover, an actual atom interferometer consists of more than one beam splitter. Since the undesired output states of the first one have different momentum, they will not be addressed by the subsequent (velocity selective) beam splitters. This strongly reduces this effect. A further reduction is possible by choosing the geometry of the interferometer such that the undesired output states do not interfere.

ACKNOWLEDGMENTS

We would like to thank an anonymous referee, as well as

B. Dubetsky, T.W. Hänsch, and Q. Long for discussions. H.M. thanks the Alexander von Humboldt foundation for support in the initial phase of this work. This material is based upon work supported by the National Science Foundation under Grant No. 0400866, the Air Force Office of Scientific Research, and the Multi-University Research Initiative.

APPENDIX A: COEFFICIENTS OF A POWER SERIES EXPANSION OF THE MATHIEU EIGENVALUES

We start from the numerical values obtained in Sec. II and make a polynomial ansatz $D_n = (n+k_1)(n+k_2)\dots$ for the denominator of the $\alpha_n^{(2j)}$. The coefficients k_i are then obtained by factoring the denominators into primes. If, for example, the prime 7 first appears at $n=7-1$ and $n=7+1$, we choose one of the k_i equal to -1 and one to $+1$. This leads to a guess for the denominator. Subsequently, an ansatz is made for the numerators N_n by a polynomial of K th order. The coefficients are determined by solving $\sum_{k=0}^K a_k n^k = N_n$ for the coefficients a_k . The resulting expression is then confirmed by direct comparison to the above calculation. As it turns out, the $\alpha_n^{(2j)}$, $n=1, 2, \dots, N$ can be given by polynomials of relatively low order compared to N . This suggests that the polynomials may turn out to be exact expressions for all n , although we have made no attempt to prove this conjecture.

The functional forms of $\beta_n^{(1)}$ and $\beta_n^{(2)}$ are obtained as follows. For $\beta_n^{(1)}$, a factorial denominator $(n-1)!$ is found, and then a recursive relation of the numerators is observed. After simplifying the relation, the functional form is obtained and tested with larger n 's. For $\beta_n^{(2)}$, ω_{-n+m} in \tilde{H} are kept not evaluated, and a pattern of the appearance of the ω 's in $\beta_n^{(2)}$ is found. The pattern is then simplified with ω 's evaluated as $\omega_{-n+2m} = m(n-m)\omega_r$, thus yields the form.

As a result, we obtain the following closed expressions for the coefficients:

$$\alpha_n^{(2)} = \frac{n+2}{2^4(n^2-1)^2}, \quad \alpha_2^{(4)} = \frac{-11\,141}{7\,077\,888},$$

$$\alpha_{n>2}^{(4)} = -(n+4)(4n^5 - 15n^4 - 32n^3 + 12n^2 + 64n + 111)/[2^{11}(n^2-1)^4(n^2-4)^2],$$

$$\alpha_2^{(6)} = \frac{1\,086\,647}{9\,555\,148\,800}, \quad \alpha_3^{(6)} = \frac{-872\,713}{1\,087\,163\,596\,800},$$

$$\alpha_{n>3}^{(6)} = (n+6)(4n^{10} - 45n^9 + 76n^8 + 846n^7 + 484n^6 - 3960n^5 - 14\,824n^4 - 3078n^3 + 31\,904n^2 + 26\,973n + 30\,740)/[3!2^{14}(n^2-1)^6(n^2-4)^2(n^2-9)^2],$$

$$\alpha_2^{(8)} = \frac{-20\,778\,032\,863}{2\,254\,342\,434\,324\,480},$$

$$\alpha_3^{(8)} = \frac{16\,738\,435\,813}{2\,727\,476\,031\,651\,840\,000},$$

$$\alpha_4^{(8)} = \frac{-218\,963\,004\,049}{2\,301\,307\,901\,706\,240\,000\,000},$$

$$\begin{aligned} \alpha_{n>4}^{(8)} = & -(n+8)(5\,191\,881\,936 + 5\,562\,082\,816n \\ & + 9\,349\,559\,664n^2 + 953\,069\,376n^3 \\ & - 6\,361\,852\,029n^4 - 3\,794\,628\,570n^5 \\ & - 375\,347\,622n^6 + 1\,490\,778\,180n^7 + 888\,115\,497n^8 \\ & - 172\,767\,750n^9 - 198\,150\,468n^{10} - 10\,966\,056n^{11} \\ & + 16\,309\,509n^{12} + 3\,762\,906n^{13} - 472\,854n^{14} \\ & - 257\,532n^{15} + 11\,487n^{16} + 4998n^{17} - 720n^{18} \\ & + 32n^{19})/[4!2^{21}(n^2-1)^8(n^2-4)^4(n^2-9)^2(n^2-16)^2], \end{aligned} \quad (\text{A1})$$

$$\beta_n^{(1)} = \frac{i}{4} \sum_{k=1}^{n-1} \frac{1}{k} \equiv \frac{i}{4} H_{n-1},$$

$$\beta_n^{(2)} = \frac{1}{16} \left[\left(1 - \frac{2}{n}\right) H_{n-1}^2 - \sum_{k=2}^{n-2} \frac{n-k-1}{k(n-k)} H_{k-1} \right]. \quad (\text{A2})$$

At present, we have proved these expressions for $n < 30$ by direct computation, as explained above. The expressions have also been checked against the differences $a_n - b_n$ of the eigenvalues of Mathieu equation, as far as they are available from [51].

APPENDIX B: MEAN OF THE EIGENVALUES a_n, b_n OF MATHIEU FUNCTIONS

Ω_{ac} , that was introduced in Eq. (39), is the common energy shift of the effective two-level system, which thus corresponds to the mean $(a_n + b_n)/2$ of characteristic values for real and constant Ω . Thus, by taking into account of the difference in energy reference in Eq. (4) and \mathcal{H} , the mean of a_n, b_n can be obtained. As a result, both a_n and b_n are known independently.

In fact, for real constant Ω , every term in the power series expansion for the mean value as a function of n can be obtained efficiently. The result is valid for all n as long as the denominator of the coefficients listed below do not vanish. This method is used to calculate the power series expansion up to the 14th order in the parameter q as introduced in Eq. (22) on a personal computer in 10 minutes, and the result agrees with Abramowitz and Stegun [51], who list the terms up to order q^6 . The subsequent terms are as follows: The coefficient of q^8 is

$$\begin{aligned} & (274\,748 + 827\,565n^2 + 64\,228n^4 - 140\,354n^6 + 9144n^8 \\ & + 1469n^{10})/[2^{21}(n^2-1)^7(n^2-4)^3(n^2-9)(n^2-16)]; \end{aligned}$$

of q^{10} ,

$$\begin{aligned} & (4\,453\,452 + 20\,651\,309n^2 + 13\,541\,915n^4 - 2\,844\,430n^6 \\ & - 1\,039\,598n^8 + 69\,361n^{10} + 4471n^{12})/[2^{24}(n^2-1)^9(n^2 \\ & - 4)^3(n^2-9)(n^2-16)(n^2-25)], \end{aligned}$$

of q^{12} ,

$$\begin{aligned} & (1\,155\,192\,131\,376 + 6\,474\,038\,960\,008n^2 \\ & + 4\,470\,328\,527\,807n^4 - 3\,667\,584\,923\,421n^6 \\ & - 518\,221\,243\,968n^8 + 604\,333\,473\,552n^{10} \\ & - 86\,398\,056\,330n^{12} - 5\,960\,020\,482n^{14} \\ & + 2\,031\,809\,256n^{16} - 119\,406\,048n^{18} - 131\,341n^{20} \\ & + 121\,191n^{22})/[2^{30}(n^2-1)^{11}(n^2-4)^5(n^2-9)^3 \\ & \times (n^2-16)(n^2-25)(n^2-36)], \end{aligned}$$

and of q^{14} ,

$$\begin{aligned} & (41\,218\,724\,372\,688 + 302\,286\,294\,466\,120n^2 \\ & + 433\,922\,366\,490\,105n^4 - 32\,881\,683\,767\,026n^6 \\ & - 136\,265\,027\,585\,703n^8 + 21\,249\,098\,173\,752n^{10} \\ & + 7\,968\,113\,847\,666n^{12} - 1\,857\,745\,713\,708n^{14} \\ & + 30\,568\,658\,442n^{16} + 15\,106\,984\,464n^{18} \\ & - 880\,061\,323n^{20} + 3\,059\,598n^{22} + 441\,325n^{24})/ \\ & [2^{33}(n^2-1)^{13}(n^2-4)^5(n^2-9)^3 \\ & \times (n^2-16)(n^2-25)(n^2-36)(n^2-49)]. \end{aligned}$$

This is the first time the close form higher-order power series expansion terms of the mean characteristic values are reported.

APPENDIX C: CALCULATION OF THE INTEGRAL

In this appendix, we calculate the integral

$$\int_{-\infty}^{\infty} dt e^{-t^2/(2\sigma^2)} \sin\left[\frac{\pi}{4} \text{erf}\left(\nu \sqrt{\frac{n}{2}} \frac{t}{\sigma}\right)\right] e^{4i(1\pm n)\omega t}.$$

We substitute $\nu \sqrt{n/2}(t/\sigma)$, to bring the integral into the form

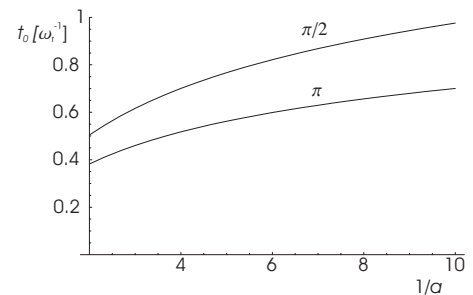


FIG. 8. t_0 for π (lower graph) as well as $\pi/2$ (upper graph) pulses, plotted versus $1/a$.

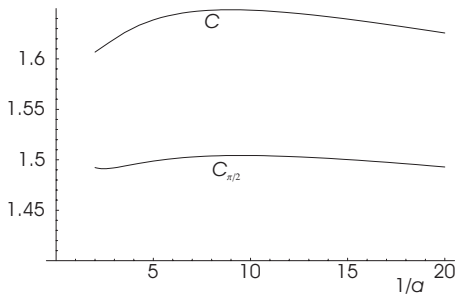


FIG. 9. C (upper graph) and $C_{\pi/2}$ (lower graph) plotted versus $1/a$.

$$g_{n\pm 2} = -i \sqrt{\frac{2\sigma^2}{n}} \frac{\bar{\Omega}}{2\nu} g_{\pm} \quad (C1)$$

where

$$g_{\pm} \equiv \int_{-\infty}^{\infty} e^{-at^2 - ibt} \sin\left(\frac{\pi}{4} \text{erp}(t)\right) dt \quad (C2)$$

and $a = 1/n$, $b = -4(1 \pm n)\sqrt{2\sigma^2/n}\omega_r/\nu$. A useful approximation is the saddle-point method. We write

$$g_{\pm} = \int_{-\infty}^{\infty} e^{f(t) - ibt} dt, \quad (C3)$$

$$f = -at^2 + \ln\left[\sin\left(\frac{\pi}{4} \text{erp}(t)\right)\right].$$

We expand into a Taylor series near the maximum of f at t_0 ,

$$g_{\pm} = \int_{-\infty}^{\infty} \exp\left\{f(t_0) + \frac{1}{2}f''(t_0)(t-t_0)^2 + \dots - ibt\right\} dt. \quad (C4)$$

Thus,

$$g = \sqrt{\frac{2\pi}{f''(t_0)}} e^{f(t_0) - ibt_0 + b^2/2f''(t_0)}. \quad (C5)$$

For finding t_0 , we calculate

$$f'(t_0) = -2at_0 + \frac{\sqrt{\pi}}{2} e^{-t_0^2} \cot\left(\frac{\pi}{4} \text{erp}(t_0)\right) = 0. \quad (C6)$$

t_0 can be calculated numerically and is plotted versus $1/a$ in Fig. 8.

For the second derivative, we calculate

$$f''(t) = -2a - e^{-t^2} \sqrt{\pi} t \cot\left(\frac{\pi}{4} \text{erp}(t_0)\right) - \frac{\pi}{4} e^{-2t^2} \csc^2\left(\frac{\pi}{4} \text{erp}(t_0)\right). \quad (C7)$$

To obtain a simplified expression for $f''(t_0)$, we derive from Eq. (C6),

$$e^{-t_0^2} \cot\left(\frac{\pi}{4} \text{erp}(t_0)\right) = \frac{4at_0}{\sqrt{\pi}},$$

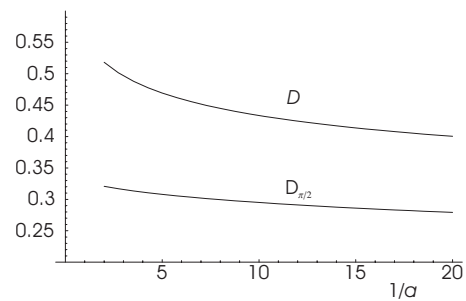


FIG. 10. The factor D (upper graph) and $D_{\pi/2}$ (lower graph) plotted versus $1/a$.

$$\csc^2\left(\frac{\pi}{4} \text{erp}(t_0)\right) = 1 + \frac{16}{\pi} a^2 t_0^2 e^{2t_0^2}. \quad (C8)$$

For obtaining the latter result, $\csc^2 x = 1 + \cot^2 x$ has been used. We obtain $f''(t_0) = -2Ca^{2/3}$ where

$$C \equiv \left(a + 2a^2 t_0^2 + \frac{\pi}{8} e^{-2t_0^2} + 2at_0^2\right) / a^{2/3}, \quad (C9)$$

t_0 as well as A depend on a only. As can be seen from Fig. 9, C is of order unity and does not vary strongly. Indeed, C has a maximum of $\Gamma \approx 1.64874$ at $1/a = 8.984$ and can be replaced by Γ with less than 3% error for $3 < 1/a < 30$.

Inserting into the expression for the integral in the saddle-point method yields

$$g_{n\pm 2} = -i \frac{\bar{\Omega} D}{\nu} \sqrt{\frac{2\sigma^2}{n}} \exp\left\{4i \frac{(1 \pm n)}{\nu} \sqrt{\frac{2\sigma^2}{n}} \omega_r t_0 - 8 \frac{(1 \pm n)^2 \sigma^2 \omega_r^2}{\nu a^{2/3} n C}\right\} = -g_{n\pm 2}^* \quad (C10)$$

The overall scaling is predominantly determined by the factor

$$\exp\left(-\frac{b^2}{4Ca^{2/3}}\right) = \exp\left(-8 \frac{(1 \pm n)^2 \sigma^2 \omega_r^2}{\nu a^{2/3} n C}\right), \quad (C11)$$

which is a strong function of σ and, thus, $\bar{\Omega}/\omega_r$. The factor

$$D \equiv \frac{1}{2} \sqrt{\frac{\pi}{Ca^{2/3}}} \sin\left[\frac{\pi}{4} \text{erp}(t_0)\right] e^{-at_0^2} \quad (C12)$$

is plotted versus $1/a$ in Fig. 10.

$\pi/2$ pulses can be treated in analogy by requiring

$$\frac{1}{2} \int \Omega_{\text{eff}}(t) dt = \frac{\pi}{4}. \quad (C13)$$

The calculation of the previous sections can be carried through in analogy, inserting factors of $1/2$. For example, Eq. (63) will have factors of $\pi/8$ in the cosine and sine

functions, rather than $\pi/4$. This means that $g_{-n\pm 2}$ will no longer be equal to $-g_{n\mp 2}^*$, so we have to treat these cases separately. In the following, we specialize on $g_{n\pm 2}$; the other ones can be treated in analogy. For the evaluation of the integral in the saddle-point method, the changes can be summarized by replacing C and thus D by

$$C_{\pi/2} \equiv \left(a + 2a^2 t_0^2 + \frac{\pi}{16} e^{-2t_0^2} + 2at_0^2 \right) / a^{2/3},$$

$$D_{\pi/2} \equiv \frac{\sqrt{\pi}}{2\sqrt{C_{\pi/2} a^{2/3}}} \sin \left[\frac{\pi}{8} \text{erp}(t_0) \right] e^{-t_0^2/n} \quad (\text{C14})$$

(note that also t_0 will have another value). $C_{\pi/2}$ has a maximum value of $\Gamma_{\pi/2} \approx 1.5043$ at $n=9.534$ and can be replaced by that value with little error for $3 \leq n \leq 30$. $D_{\pi/2}$ is also plotted in Fig. 10. It is a slowly varying function of n with a value somewhat lower than that for π pulses. However, in general losses for $\pi/2$ pulses will be higher, because of the lower σ that enters the exponential which chiefly determines the magnitude.

-
- [1] C. Keller, J. Schmiedmayer, A. Zeilinger, T. Nonn, S. Dürr, and G. Rempe, *Appl. Phys. B: Lasers Opt.* **69**, 303 (1999).
- [2] M. Buchner, R. Delhuille, A. Miffre, C. Robilliard, J. Vigue, and C. Champenois, *Phys. Rev. A* **68**, 013607 (2003).
- [3] P. C. D. Hobbs, *Building Electro-Optical Systems* (Wiley, New York, 2000).
- [4] *Optische Kommunikationstechnik*, edited by E. Voges and K. Petermann (Springer, Berlin, 2002).
- [5] Henry M. van Driel and Willem L. Vos, *Phys. Rev. B* **62**, 9872 (2000).
- [6] P. Kapitza and P. A. M. Dirac, *Proc. Cambridge Philos. Soc.* **29**, 297 (1933).
- [7] S. Althshule, L. Frantz, R. Braunste, *Phys. Rev. Lett.* **17**, 231 (1966).
- [8] P. J. Martin, B. G. Oldaker, A. H. Milklich, and D. E. Pritchard, *Phys. Rev. Lett.* **60**, 515 (1988).
- [9] P. R. Berman and B. Bian, *Phys. Rev. A* **55**, 4382 (1997).
- [10] H. Batelaan, *Contemp. Phys.* **41**, 369 (2000).
- [11] S. Gupta, A. E. Leanhardt, A. D. Cronin, and D. E. Pritchard, *C. R. Acad. Sci., Ser. IV Phys. Astrophys.* **2**, 479 (2001).
- [12] S. Gupta, K. Dieckmann, Z. Hadzibabic, and D. E. Pritchard, *Phys. Rev. Lett.* **89**, 140401 (2002).
- [13] O. Morsch and M. Oberthaler, *Rev. Mod. Phys.* **78**, 179 (2006).
- [14] M. Kozuma, L. Deng, E. W. Hagley, J. Wen, R. Lutwak, K. Helmerson, S. L. Rolston, and W. D. Phillips, *Phys. Rev. Lett.* **82**, 871 (1999).
- [15] A. T. Black, H. W. Chan, and V. Vuletic, *Phys. Rev. Lett.* **91**, 203001 (2003).
- [16] Pierre Meystre, *Atom Optics* (Springer, Berlin, 2001).
- [17] S. Bernet, M. Oberthaler, R. Abfalterer, J. Schmiedmayer and A. Zeilinger, *Quantum Semiclass. Opt.* **8**, 497 (1996).
- [18] S. Wu, Y. Wang, Q. Diot, and M. Prentiss, *Phys. Rev. A* **71**, 043602 (2005).
- [19] C. J. Bordé and C. Lämmerzahl, *Ann. Phys.* **8**, 83 (1999).
- [20] Vladimir S. Malinovsky and Paul R. Berman, *Phys. Rev. A* **68**, 023610 (2003).
- [21] A. E. A. Koolen, G. T. Jansen, K. F. E. M. Domen, H. C. W. Beijerinck, and K. A. H. van Leeuwen, *Phys. Rev. A* **65**, 041601(R) (2002).
- [22] D. M. Giltner, R. W. McGowan, and S. A. Lee, *Phys. Rev. Lett.* **75**, 2638 (1995).
- [23] D. M. Giltner, R. W. McGowan, and S. A. Lee, *Phys. Rev. A* **52**, 3966 (1995).
- [24] D. E. Miller, J. R. Anglin, J. R. Abo-Shaeer, K. Xu, J. K. Chin, and W. Ketterle, *Phys. Rev. A* **71**, 043615 (2005).
- [25] Yoshio Torii, Yoichi Suzuki, Mikio Kozuma, Toshiaki Sugiura, Takahiro Kuga, Lu Deng, and E. W. Hagley, *Phys. Rev. A* **61**, 041602(R) (2000).
- [26] E. M. Rasel, M. K. Oberthaler, H. Batelaan, J. Schmiedmayer, and A. Zeilinger, *Phys. Rev. Lett.* **75**, 2633 (1995).
- [27] C. R. Ekstrom, J. Schmiedmayer, M. S. Chapman, T. D. Hammond, and D. E. Pritchard, *Phys. Rev. A* **51**, 3883 (1995).
- [28] A. Miffre, M. Jacquey, M. Büchner, G. Trenec, and J. Vigue, *Phys. Rev. A* **73**, 011603(R) (2006).
- [29] J. Schmiedmayer, M. S. Chapman, C. R. Ekstrom, T. D. Hammond, S. Wehinger, and D. E. Pritchard, *Phys. Rev. Lett.* **74**, 1043 (1995).
- [30] A. Peters, K. Y. Chung, and S. Chu, *Nature (London)* **400**, 849 (1999).
- [31] J. Stuhler, M. Fattori, T. Petelski, and G. M. Tino, *J. Opt. B: Quantum Semiclassical Opt.* **5**, S75 (2003).
- [32] S. Dimopoulos, P. W. Graham, J. M. Hogan, and M. A. Kasevich, *Phys. Rev. Lett.* **98**, 111102 (2007).
- [33] A. Wicht, J. M. Hensley, E. Sarajlic, and S. Chu, *Phys. Scr., T* **102**, 82 (2002).
- [34] P. Clade, E. de Mirandes, M. Cadoret, S. Guellati-Khelifa, C. Schwob, F. Nez, L. Julien, and F. Biraben, *Phys. Rev. Lett.* **96**, 033001 (2006).
- [35] Holger Müller, Sheng-wei Chiow, Quan Long, Christoph Vo, and Steven Chu, *Appl. Phys. B: Lasers Opt.* **84**, 633 (2006).
- [36] Y. Le Coq, J. A. Retter, S. Richard, A. Aspect, and P. Bouyer, *Appl. Phys. B: Lasers Opt.* **84**, 627 (2006).
- [37] N. Yu, J. M. Kohel, J. R. Kellogg, and L. Maleki, *Appl. Phys. B: Lasers Opt.* **84**, 647 (2006).
- [38] J. M. McGuirk, M. J. Snadden, and M. A. Kasevich, *Phys. Rev. Lett.* **85**, 4498 (2000).
- [39] B. Dubetsky and P. R. Berman, *Phys. Rev. A* **56**, R1091 (1997).
- [40] T. Pfau, Ch. Kurtsiefer, C. S. Adams, M. Sigel, and J. Mlynek, *Phys. Rev. Lett.* **71**, 3427 (1993).
- [41] H. Müller, S-w. Chiow, Q. Long, and S. Chu, *Opt. Lett.* **31**, 202 (2006).
- [42] S. Dürr and G. Rempe, *Phys. Rev. A* **59**, 1495 (1999).
- [43] J. Stenger, S. Inouye, D. M. Stamper-Kurn, A. P. Chikkatur, D. E. Pritchard, and W. Ketterle, *Appl. Phys. B: Lasers Opt.* **69**, 347 (1999).
- [44] E. Peik, M. Ben Dahan, I. Bouchoule, Y. Castin, and C.

- Salomon, Phys. Rev. A **55**, 2989 (1997).
- [45] Y. B. Band, Marek Trippenbach, J. P. Burke, Jr., and P. S. Julienne, Phys. Rev. Lett. **84**, 5462 (2000).
- [46] P. B. Blakie and R. J. Ballagh, Phys. Rev. Lett. **86**, 3930 (2001).
- [47] S. Dürr, S. Kunze, and G. Rempe, Quantum Semiclassic. Opt. **8**, 531 (1996).
- [48] C. Champenois, M. Buchner, R. Dehuille, R. Mathevet, C. Robillard, C. Rizzo, and J. Vigue, Eur. Phys. J. D **13**, 271 (2001).
- [49] M. Horne, I. Jex, and A. Zeilinger, Phys. Rev. A **59**, 2190 (1999).
- [50] G. C. Kokkorakis and J. A. Roumelotis, Math. Comput. **70**, 1221 (2000).
- [51] M. Abramowitz and I. A. Stegun, *Handbook of Mathematical Functions* (Dover, New York, 1965).
- [52] I. S. Gradshteyn and I. M. Rhyshik, *Table of Integrals, Series, and Products*, 6th ed. (Academic Press, San Diego, 2000).
- [53] This condition also ensures that the argument of Ω_{eff} changes adiabatically, and that the overall phase factor $e^{-i\varphi}$ specified in Sec. I E 2 can be neglected, as $\varphi \ll 1$.
- [54] D. A. Steck, Cesium D line data, available at <http://steck.us/alkalidata> (updated about twice a year).
- [55] B. Dubetsky and P. Berman, Phys. Rev. A **64**, 063612 (2001).
- [56] B. Dubetsky and G. Raithel, e-print arXiv:physics/0206029v1.